Intramolecular Hydrophosphination/Cyclization of Phosphinoalkenes and Phosphinoalkynes Catalyzed by Organolanthanides: Scope, Selectivity, and Mechanism

Michael R. Douglass, Charlotte L. Stern, and Tobin J. Marks*

Contribution from the Department of Chemistry, Northwestern University, Evanston, Illinois 60208-3113

Received March 28, 2001

Abstract: Organolanthanide complexes of the general type $Cp'_2LnE(TMS)_2$ ($Cp' = \eta^5$-Me_5C_5; Ln = La, Sm, Y, Lu; E = CH, N; TMS = $SiMe_3$) serve as effective precatalysts for the rapid intramolecular hydrophosphination/cyclization of the phosphinoalkenes and phosphinoalkynes $RHP(CH_2)_nCH{=}CH_2$ (R = Ph, H; n = 3, 4) and $H_2P(CH_2)_nC{\equiv}C{-}Ph$ (n = 3, 4) to afford the corresponding heterocycles $CH_3\overline{CH(CH_2)_nPR}$ and $Ph(H)C{=}\overline{C(CH_2)_nPH}$, respectively. Kinetic and mechanistic data for these processes exhibit parallels to, as well as distinct differences from, organolanthanide-mediated intramolecular hydroamination/cyclizations. The turnover-limiting step of the present catalytic cycle is insertion of the carbon−carbon unsaturation into the Ln−P bond, followed by rapid protonolysis of the resulting Ln−C linkage. The rate law is first-order in [catalyst] and zero-order in [substrate] over approximately one half-life, with inhibition by heterocyclic product intruding at higher conversions. The catalyst resting state is likely a lanthanocene phosphine−phosphido complex, and dimeric $[Cp'_2YP(H)Ph]_2$ was isolated and cystallographically characterized. Lanthanide identity and ancillary ligand structure effects on rate and selectivity vary with substrate unsaturation: larger metal ions and more open ligand systems lead to higher turnover frequencies for phosphinoalkynes, and intermediate-sized metal ions with Cp'_2 ligands lead to maximum turnover frequencies for phosphinoalkenes. Diastereoselectivity patterns also vary with substrate, lanthanide ion, and ancillary ligands. Similarities and differences in hydrophosphination vis-à-vis analogous organolanthanide-mediated hydroamination are enumerated.

Introduction

The use of organolanthanide catalysts to effect a wide variety of synthetically useful catalytic reactions is rapidly growing in scope and diversity.[1] Variation of the metal ionic radius,[2] as well as the wide variety of available nondisassociable ancillary ligands compatible with lanthanide metal centers,[3−5] renders this area of catalysis uniquely applicable to a host of new and potentially useful transformations. Organolanthanides have been applied successfully to the chemo-, regio-, and enantioselective catalytic hydrogenation of olefins, alkynes, and imines,[6] hydrosilylation of olefins and alkynes,[7] hydroboration of olefins,[8] various types of polymerizations and copolymerizations,[5,9] and in particular to the hydroamination/cyclization/bicyclization of aminoalkenes,[10,11] aminoalkynes,[12] and aminoallenes.[13] The

(1) For organolanthanide reviews, see: (a) Molander, G. A. *Chemtracts: Org. Chem.* **1998**, *18*, 237−263. (b) Edelmann, F. T. *Top. Curr. Chem.* **1996**, *179*, 247−276. (c) Edelmann, F. T. In *Comprehensive Organometallic Chemistry*; Wilkinson, G., Stone, F. G. A., Abel, E. W., Eds.; Pergamon Press: Oxford, U.K., 1995; Vol. 4, Chapter 2. (d) Schumann, H.; Meese-Marktscheffel, J. A.; Esser, L. *Chem. Rev.* **1995**, *95*, 865−986. (e) Schaverien, C. J. *Adv. Organomet. Chem.* **1994**, *36*, 283−362. (f) Evans, W. J. *Adv. Organomet. Chem.* **1985**, *24*, 131−177. (g) Marks, T. J.; Ernst, R. D. In *Comprehensive Organometallic Chemistry*; Wilkinson, G., Stone, F. G. A., Abel, E. W., Eds.; Pergamon Press: Oxford, U.K., 1982, Chapter 21.

(2) Shannon, R. D. *Acta Crystallogr.* **1976**, *A32*, 751−760.

(3) a) CGC complexes: (a) Tian, S.; Arredondo, V. A.; Stern, C. L.; Marks, T. J. *Organometallics* **1999**, *18*, 2568−2570. (b) Shapiro, P. J.; Cotter, M. D.; Schaefer, W. P.; Labinger, J. A.; Bercaw, J. E. *J. Am. Chem. Soc.* **1994**, *116*, 4623−4640.

(4) Chiral auxiliaries: (a) Giardello, M. A.; Conticello, V. P.; Brard, L.; Sabat, M.; Rheingold, A. L.; Stern, C.; Marks, T. J. *J. Am. Chem. Soc.* **1994**, *116*, 10012−10040. (b) Giardello, M. A.; Conticello, V. P.; Brard, L.; Gagné, M. R.; Marks, T. J. *J. Am. Chem. Soc.* **1994**, *116*, 10241−10254. (c) Douglass, M. R.; Ogasawara, M.; Metz, M. V.; Marks, T. J. *Organometallics*, in press.

(5) (a) Bis-Cp′ alkyl and hydride complexes: Jeske, G.; Lauke, H.; Mauermann, H.; Swepston, P. N.; Schumann, H.; Marks, T. J. *J. Am. Chem. Soc.* **1985**, *107*, 8091−8103. (b) Si-bridged and mixed Cp complexes: Jeske, G.; Schock, L. E.; Mauermann, H.; Swepston, P. N.; Schumann, H.; Marks, T. J. *J. Am. Chem. Soc.* **1985**, *107*, 8103−8110.

(6) Hydrogenation: (a) Obora, Y.; Ohta, T.; Stern, C. L.; Marks, T. J. *J. Am. Chem. Soc.* **1997**, *119*, 3745−3755. (b) Roesky, P. W.; Denninger, U.; Stern, C. L.; Marks, T. J. *Organometallics* **1997**, *16*, 4486-4492. (c) Haar, C. M.; Stern, C. L.; Marks, T. J. *Organometallics* **1996**, *15*, 1765−1784. (d) Reference 5a.

(7) Hydrosilylation: (a) Molander, G. A.; Corrette, C. P. *Organometallics* **1998**, *17*, 5504−5512. (b) Schumann, H.; Keitsch, M. R.; Winterfeld, J.; Muhle, S.; Molander, G. A. *J. Organomet. Chem.* **1998**, *559*, 181−190. (c) Fu, P.-F.; Brard, L.; Li, Y.; Marks, T. J. *J. Am. Chem. Soc.* **1995**, *117*, 7157−7168. (d) Molander, G. A.; Julius, M. *J. Org. Chem.* **1992**, *57*, 6347−6351. (e) Sakakura, T.; Lautenschlager, H.; Tanaka, M. *J. Chem. Soc., Chem. Commun.* **1991**, 40−41.

(8) Hydroboration: (a) Molander, G. A.; Pfeiffer, D. *Org. Lett.* **2001**, *3*, 361−363. (b) Bijpost, E. A.; Duchateau, R.; Teuben, J. H. *J. Mol. Catal.* **1995**, *95*, 121−128. (c) Harrison, K. N.; Marks, T. J. *J. Am. Chem. Soc.* **1992**, *114*, 9220−9221.

(9) (a) Koo, K.; Fu, P.-F.; Marks, T. J. *Macromolecules* **1999**, *32*, 981−988. (b) Jia, L.; Yang, X.; Seyam, A. M.; Albert, I. D. L.; Fu, P.-F.; Yang, S.; Marks, T. J. *J. Am. Chem. Soc.* **1996**, *118*, 7900−7913. (c) Watson, P. L. *J. Am. Chem. Soc.* **1982**, *104*, 337−339.

(10) (a) Ryu, J.-S.; McDonald, F. E.; Marks, T. J. *Org. Lett.* **2001**, in press. (b) Molander, G. A.; Dowdy, E. D. *J. Org. Chem.* **1999**, *64*, 6515−6517. (c) Molander, G. A.; Dowdy, E. D. *J. Org. Chem.* **1998**, *63*, 8983−8988. (d) Kim, Y. K.; Livinghouse, T.; Bercaw, J. E. *Tetrahedron Lett.* **2001**, *42*, 2933−2935.

(11) (a) Gagné, M. R.; Stern, C. L.; Marks, T. J. *J. Am. Chem. Soc.* **1992**, *114*, 275−294. (b) Gagné, M. R.; Marks, T. J. *J. Am. Chem. Soc.* **1989**, *111*, 1, 4108−4109. (c) Reference 4b.

10.1021/ja010811i CCC: $20.00
Published on Web 09/26/2001

success of the various types of hydro-elementation processes catalyzed by organolanthanides raises the intriguing question of whether analogous addition/cyclization processes are possible for phosphorus-containing substrates. Olefin hydrophosphination has proven generally difficult to accomplish with typical late transition metal catalysts.[14] However, the aforementioned stereoelectronic tunability of organolanthanide coordination spheres, coupled with high electrophilicity, absence of conventional oxidative-addition/reductive-elimination pathways, and high kinetic lability, offers an attractive alternative pathway for accomplishing this transformation. Cyclic phosphines are as yet understudied,[15] and may have applications as ligands similar to all-carbon ligands[16] or display interesting pharmacological properties.[17] In addition, phosphorus heterocycles produced in hydrophosphination/cyclization processes offer attractive building blocks for classes of electron-rich chiral ligands (e.g., **A**, **B**) that have been utilized extensively for a variety of asymmetric transformations.[18] Thus, organolanthanide-catalyzed hydrophosphination could afford new synthetic routes to both existing and new classes of ligands.

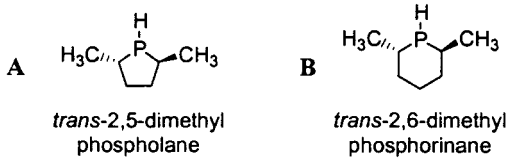

trans-2,5-dimethyl phospholane

trans-2,6-dimethyl phosphorinane

The catalytic cycle for organolanthanide-mediated hydroamination/cyclization of amine substrates is mechanistically and thermochemically reasonably well-defined (Scheme 1).[11−13] After immediate and quantitative protonolysis of the hydrocarbyl or amido precatalyst (Scheme 1, step *i*), the first step is turnover-limiting insertion of the carbon−carbon unsaturation into the lanthanide−nitrogen bond (Scheme 1, step *ii*). The second step is facile intermolecular or intramolecular protonolysis of the lanthanide−carbon bond by substrate, releasing the nitrogen-containing heterocyclic product and regenerating a lanthanide−nitrogen bond (Scheme 1, step *iii*). Thermodynamic estimates support the viability of this cycle ($\Delta H \approx -13$ kcal/mol for alkenes, -35 kcal/mol for alkynes), and the broad scope of the process, including construction of alkaloid natural products,[13b] has been demonstrated. Analogous thermodynamic analysis[19] for phosphines indicates that a similar catalytic cycle should be possible, in that after initial protonlysis of the precatalyst (Scheme 2, step *i*), insertion of a carbon−carbon unsaturation into a lanthanide−phosphorus bond (Scheme 2, step *ii*) should be exothermic for alkynes ($\Delta H \approx -33$ kcal/mol) or approximately thermoneutral for alkenes ($\Delta H \approx +2$ kcal/mol). When coupled with subsequent protonolysis (Scheme 2, step

Scheme 1. Simplified Catalytic Cycle for Organolanthanide-Mediated Hydroamination/Cyclization of Aminoalkenes and Aminoalkynes

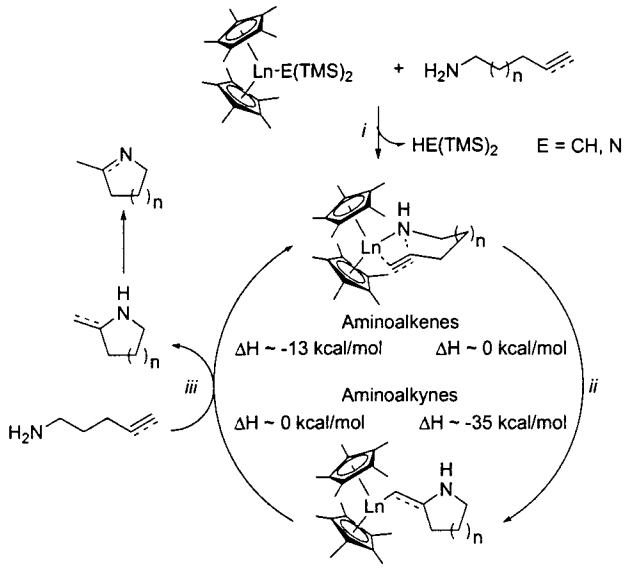

Scheme 2. Proposed Catalytic Cycle for Organolanthanide-Mediated Hydrophosphination/Cyclization of Phosphinoalkenes and Phosphinoalkynes

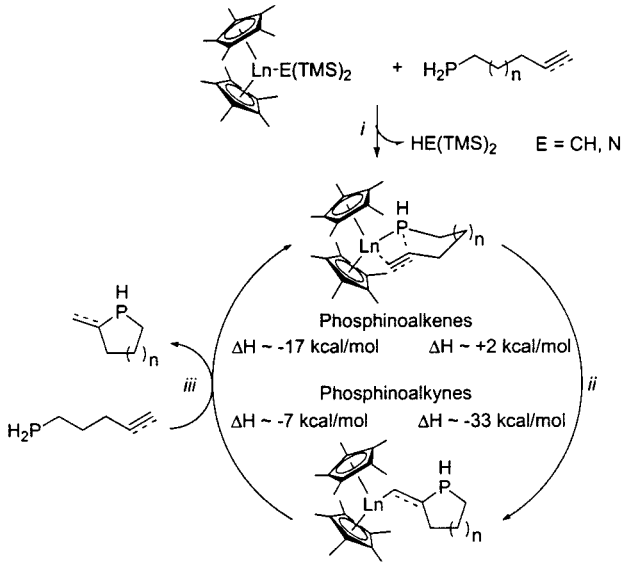

(12) (a) Li, Y.; Marks, T. J. *J. Am. Chem. Soc.* **1998**, *120*, 1757−1771. (b) Li, Y.; Marks, T. J. *J. Am. Chem. Soc.* **1996**, *118*, 9295−9306. (c) Li, Y.; Marks, T. J. *Organometallics* **1996**, *15*, 3370−3372. (d) Li, Y.; Marks, T. J. *J. Am. Chem. Soc.* **1996**, *118*, 707−708. (e) Li, Y.; Fu, P.-F.; Marks, T. J. *Organometallics* **1994**, *13*, 439−440.

(13) (a) Arredondo, V. A.; McDonald, F. M.; Marks, T. J. *Organometallics* **1999**, *10*, 1949−1960. (b) Arredondo, V. A.; Tian, S.; McDonald, F. M.; Marks, T. J. *J. Am. Chem. Soc.* **1999**, *121*, 3633−3639. (c) Arredondo, V. A.; McDonald, F. M.; Marks, T. J. *J. Am. Chem. Soc.* **1998**, *120*, 4871−4872.

(14) Hydrophosphination mediated by Pd, Pt, Ni complexes: (a) Kovacik, I.; Wicht, D. K.; Grewal, N. S.; Glueck, D. S.; Incarvito, C. D.; Guzei, I. A.; Rheingold, A. L. *Organometallics* **2000**, *19*, 950−953. (b) Wicht, D. K.; Kourkine, I. V.; Kovacik, I.; Glueck, D. S.; Concolina, T. E.; Yap, G. P. A.; Incarvito, C. D.; Rheingold, A. L. *Organometallics* **1999**, *18*, 5381−5394. (c) Costa, E.; Pringle, P. G.; Worboys, K. *Chem. Commun.* **1998**, 49−50. (d) Wicht, D. K.; Kourkine, I. V.; Lew, B. M.; Nthenge, J. M.; Glueck, D. S. *J. Am. Chem. Soc.* **1997**, *119*, 5039−5040. (e) Han, L.-B.; Tanaka, M. *J. Am. Chem. Soc.* **1996**, *118*, 1571−1572. (f) Using no transition metal catalyst: Gaumont, A.-C.; Simon, A.; Denis, J.-M. *Tetrahedron Lett.* **1998**, *39*, 985−988.

(15) a) Quin, L. D.; Hughes, A. N. In *The Chemistry of Organophosphorus Compounds*; Hartley, F. R., Ed.; Wiley: Chichester, 1990; Vol. 1, pp 295−394. (b) Quin, L. D. *The Heterocyclic Chemistry of Phosphorus: Systems Based on the Phosphorus−Carbon Bond*; Wiley: New York, 1981.

(16) Dillon, K. B.; Mathey, F.; Nixon, J. F. *Phosphorus: The Carbon Copy*; Wiley: Chichester, 1998.

(17) Price, N. R.; Chambers, J. In *The Chemistry of Organophosphorus Compounds*; Hartley, F. R., Ed.; Wiley: Chichester, 1990; Vol. 1, pp 643−661.

(18) (a) Burk, M. J. *Acc. Chem. Res.* **2000**, *33*, 363−372. (b) Burk, M. J.; Gross, M. F.; Martinez, J. P. *J. Am. Chem. Soc.* **1995**, *117*, 9375−9376. (c) Burk, M. J.; Harper, G. P.; Kalberg, C. S. *J. Am. Chem. Soc.* **1995**, *117*, 4423−4424. (d) Burk, M. J.; Feaster, J. E.; Nugent, W. A.; Harlow, R. L. *J. Am. Chem. Soc.* **1993**, *115*, 10125−10138.

(19) Bond enthalpy data: (a) Nolan, S. P.; Stern, D.; Hedden, D.; Marks, T. J. *ACS Symp. Ser.* **1990**, *428*, 159−174. (b) Nolan, S. P.; Stern, D.; Marks, T. J. *J. Am. Chem. Soc.* **1989**, *111*, 7844−7853. (c) Skinner, H. A.; Pilcher, G. In *The Chemistry of the Metal-Carbon Bond*; Hartley, F. R., Patai, S., Eds.; John Wiley & Sons: Chichester, 1982; Vol. 1, Chapter 2. (d) Goldwhite, H. *Introduction to Phosphorus Chemistry*; Cambridge University Press: Cambridge, 1981.

iii, $\Delta H \approx -7$ kcal/mol for alkynes, -17 kcal/mol for alkenes), the data indicate a thermodynamically feasible process.[20] Indeed, a preliminary investigation indicated that organolanthanide-mediated hydrophosphination is a viable process.[21] Herein we report a full discussion of reaction scope, metal and ancillary ligand effects, regio- and diastereoselectivity, and kinetics and mechanism for several series of phosphinoalkenes and phosphinoalkynes. It will be seen that organolanthanide-catalyzed hydrophosphination/cyclization has a broad scope, that variation of the metal and ligands has significant and understandable influence on the catalytic process, that the chemo-, regio-, and stereoselectivity of the process can be controlled to a significant degree, and that the kinetics and mechanism are in some ways similar to, and in some ways different significantly from, those established for hydroamination.[11−13]

Experimental Section

Materials and Methods. All manipulations of air-sensitive materials were carried out with rigorous exclusion of oxygen and moisture in flame- or oven-dried Schlenk-type glassware on a dual-manifold Schlenk line, or interfaced to a high-vacuum line (10^{-6} Torr), or in a nitrogen-filled Vacuum Atmospheres glovebox with a high-capacity recirculator (<1 ppm of O_2). Argon (Matheson, prepurified) was purified by passage through a MnO oxygen-removal column and a Davison 4 Å molecular sieve column. The solvents, ether and THF, were distilled before use from appropriate drying agents (sodium benzophenone ketyl, metal hydrides, Na/K alloy) under nitrogen. The solvents, pentane and toluene, were dried using activated alumina columns according to the method described by Grubbs[22] and were additionally vacuum-transferred from Na/K alloy immediately before use if employed for catalyst synthesis or catalytic reactions. Deuterated solvents (Cambridge Isotope Laboratories; all 99+ atom % D) used for NMR reactions and kinetic measurements (benzene-d_6 and toluene-d_8) were stored in vacuo over Na/K alloy in resealable bulbs and were vacuum-transferred immediately prior to use. All organic starting materials were purchased from Aldrich Chemical Co., Farchan Laboratories Inc., or Lancaster Synthesis Inc. and were used without further purification unless otherwise stated. All substrates were dried a minimum of two times as solutions in benzene-d_6 or toluene-d_8 over freshly activated Davison 4 Å molecular sieves and were degassed by freeze−pump−thaw methods. They were then stored in vacuum-tight storage flasks. Solutions of alkenyl phosphines were protected from light to minimize endocyclization reactions. Concentrations of substrate solutions were determined by NMR integration after addition of a known volume of solution to a precatalyst. The organolanthanide precatalysts $Cp'_2LnCH(TMS)_2$ (Ln = La, Sm, Y, Lu; $Cp' = \eta^5$-Me_5C_5),[5] $Me_2Si(Me_4C_5)(^tBuN)SmN(TMS)_2$,[3a] and $Me_2Si(Cp'')(CpR^*)LnCH(TMS)_2$ ($Cp'' = C_5Me_4$, R* = (−)-menthyl, (+)-neomenthyl)[4a] were prepared by published procedures.

Physical and Analytical Measurements. NMR spectra were recorded on either a Varian Gemini-300 (FT, 300 MHz, ^{1}H; 75 MHz, ^{13}C; 121 MHz, ^{31}P), Unity- or Mercury-400 (FT, 400 MHz, ^{1}H; 100 MHz, ^{13}C; 162 MHz, ^{31}P), or Inova-500 (FT, 500 MHz, ^{1}H; 125 MHz, ^{13}C; 202 MHz, ^{31}P) instrument. Chemical shifts (δ) for ^{1}H and ^{13}C are referenced to internal solvent resonances and reported relative to $SiMe_4$. Chemical shifts for ^{31}P are reported relative to an external 85% H_3PO_4 standard. NMR experiments with air-sensitive samples were conducted in Teflon valve-sealed tubes (J. Young). HRMS studies were conducted on a VG 70-250 SE instrument with 70 eV electron impact ionization for substrates containing a phenyl group, and atmospheric pressure chemical ionization for primary phosphines and the products of their cyclizations, which were too volatile to be analyzed using EI. Elemental analyses were carried out by Midwest Microlabs, Indianapolis, IN.

Synthesis of Pent-4-enylphosphine (1). Diethyl-4-pentenylphosphonate (1a). The reagent 5-bromo-1-pentene (9.4 mL, 79.5 mmol) was subjected to reaction with $P(OEt)_3$ (15.0 mL, 87.5 mmol) at 150 °C overnight, and the resulting phosphonate was purified by distillation (55 °C/0.08 Torr) to yield a colorless oil (11.5 g, 70.5% yield). ^{1}H NMR (300 MHz, C_6D_6): δ 5.57 (m, 1H), 4.93 (m, 2H), 3.90 (m, 4H), 1.90 (q, 6.6 Hz, 2H), 1.61 (m, 4H), 1.04 (t, 7.2 Hz, 6H); ^{13}C NMR (75 MHz, C_6D_6): δ 138.2, 115.9, 61.4 (d, 6.1 Hz), 35.0, 34.8, 26.9, 25.0, 22.6 (d, 4.6), 17.0 (d, 5.3); ^{31}P NMR (121 MHz, C_6D_6): δ 32.3. HRMS (*m*/*z*): [M^+] calcd for $C_9H_{19}O_3P$, 206.1072; found, 206.10715. Anal. Calcd for $C_9H_{19}O_3P$: C, 52.40; H, 9.29. Found: C, 52.24; H, 9.20.

Pent-4-enylphosphine (1b). The reducing agent $AlCl_2H$ was generated in situ from $AlCl_3$ (6.48 g, 48.5 mmol) and $LiAlH_4$ (0.74 g, 19.5 mmol) in 50 mL of tetraglyme (vacuum-distilled from Na twice).[23,24] The tetraglyme was added to the $LiAlH_4$ powder, and then the $AlCl_3$ solid was added under an N_2 flush at 0 °C in several portions. (Addition of tetraglyme to $AlCl_3$ results in an intractable black solid; therefore, the order of reagent addition is critical in forming this reducing agent in tetraglyme.) Next, phosphonate **1a** (2.0 g, 9.7 mmol) was added to the $AlCl_2H$ solution via syringe (an exotherm was observed), and the reaction mixture was stirred until the reduction was complete by ^{31}P NMR (ca. 1 h). Deoxygenated water was then added slowly via cannula at 0 °C until a clear upper layer separated from a lower gray aqueous layer. The upper layer was separated via cannula and degassed, and phosphine **1b** was vacuum-transferred away from the tetraglyme solution into a storage tube (cooled to −78 °C) containing activated 4 Å molecular sieves and C_6D_6. The final solution concentration was ~1 M by NMR, indicating an approximately 50% yield. ^{1}H NMR (300 MHz, C_6D_6): δ 5.6 (m, 1 H), 4.95−4.91 (m, 2H), 2.47 (d of t, 190.5 Hz, 2H), 1.84 (q, 7.0 Hz, 2H), 1.32 (qu, 7.5 Hz, 2H), 1.13 (m, 2H); ^{13}C NMR (75 MHz, C_6D_6): δ 138.6, 115.5, 35.2 (d, 5.2 Hz), 32.9 (d, 3 Hz), 13.7 (d, 8.3 Hz); ^{31}P NMR (121 MHz, C_6D_6): δ −137.8 (t, $^1J_{P-H}$ = 190 Hz). HRMS (*m*/*z*): [MH^+] calcd for $C_5H_{12}P$, 103.0625; found, 103.0607.

Synthesis of 1-Methylpent-4-enylphosphine (3). Diethyl-1-methylpent-4-enylphosphonate (3a). The reagent diethyl ethylphosphonate (8.66 g, 52.2 mmol) was treated with *n*-BuLi (1.6 M, 62.6 mmol, 39.1 mL) in 50 mL of THF at −45 °C for 30 min. Next, 4-bromo-1-butene (5.56 mL, 54.8 mmol) was added dropwise, and the solution was allowed to warm to room temperature and stirred for an additional 2.5 h, turning yellow and then orange during this time. The reaction was then quenched with water, dried with brine and $MgSO_4$ and filtered, and the solvent was removed in vacuo. Distillation of the resulting phosphonate (145 °C/12 Torr) afforded a colorless oil in approximately 60% yield. ^{1}H NMR (500 MHz, C_6D_6): δ 5.67 (m, 1H), 4.97 (m, 2H), 3.93 (m, 4H), 2.12 (m, 1H), 1.97 (m, 2H), 1.75 (m, 1H), 1.46 (m, 1H), 1.12 (d of d, 18 Hz, 7.0 Hz, 3H), 1.04 (t, 7.0 Hz, 6H); ^{13}C NMR (125 MHz, C_6D_6): δ 138.6, 115.6, 61.5 (t, 6.8 Hz), 32.0 (d, 12.5 Hz), 31.6, 30.4, 30.2 (d, 3.5 Hz), 17.0 (d, 5.0 Hz), 13.8 (d, 5.0 Hz); ^{31}P NMR (162 MHz, C_6D_6): δ 35.2. HRMS (*m*/*z*): [M^+] calcd for $C_{10}H_{21}O_3P$, 220.1228; found, 220.1227. Anal. Calcd for $C_{10}H_{21}O_3P$: C, 54.53; H, 9.61. Found: C, 54.56; H, 9.80.

1-Methylpent-4-enylphosphine (3b). The phosphonate **3a** was reduced using $AlCl_2H$ in tetraglyme as described for **1b**, and the resulting phosphine **3b** was vacuum-transferred away from the tetraglyme solution into a storage tube (cooled to −78 °C) containing activated 4 Å molecular sieves and C_6D_6. The final solution concentration was ~1 M by NMR, indicating an approximately 50% yield. ^{1}H NMR (400 MHz, C_6D_6): δ 5.63 (m, 1 H), 4.96 (m, 2H), 2.63 (d of m, 189.2 Hz, 2H), 1.94 (q, 7.0 Hz, 2H), 1.58 (sept, 6.8 Hz, 1H), 1.32 (m, 2H), 0.96, (d of d, 12.4 Hz, 7.2 Hz, 3H); ^{13}C NMR (125 MHz, C_6D_6): δ 138.7, 115.3, 39.1 (d, 10.4 Hz), 33.3 (d, 9.5 Hz), 23.7 (d, 10.0 Hz),

(20) AM-1 level calculations corroborate the thermodynamic estimates, and indicate that addition of methyl phosphine to ethylene is exothermic by ~−15 kcal/mol, while addition to acetylene is exothermic by ~−38 kcal/mol. We thank Dr. A. Israel for these calculations.

(21) (a) Douglass, M. R.; Marks, T. J. *J. Am. Chem. Soc.* **2000**, *122*, 1824−1825. (b) Douglass, M. R.; Marks, T. J. Communicated in part at the 217th National Meeting of the American Chemical Society, Anaheim, CA, March 1999; Abstract INOR 375. (c) Preliminary observations: Giardello, M. A.; King, W. A.; Nolan, S. P.; Porchia, M.; Sishta, C.; Marks, T. J. In *Energetics of Organometallic Species;* Marthinho Simoes, J. A., Ed.; Kluwer: Dordrecht, 1992; pp 35−51.

(22) Pangborn, A. B.; Giardello, M. A.; Grubbs, R. H.; Rosen, R. K.; Timmers, F. J. *Organometallics* **1996**, *15*, 1518−1520.

(23) Guillemin, J. C.; Savignac, P.; Denis, J.-M. *Inorg. Chem.* **1991**, *30*, 2170−2173.

(24) Ashby, E. C.; Prather, J. *J. Am. Chem. Soc.* **1966**, *88*, 729−733.

22.6 (d, 7.0 Hz); ^{31}P NMR (121 MHz, C_6D_6): δ −111.8 (t, $^1J_{P-H}$ = 188.5 Hz). HRMS (*m*/*z*): [MH$^+$] calcd for $C_6H_{14}P$, 117.0828; found, 117.0807.

Synthesis of Hex-5-enylphosphine (5). Dimethyl-hex-5-enylphosphonate (5a). To a solution of *n*-BuLi (1.6 M, 80.5 mmol, 50.3 mL) in THF (100 mL) at −45 °C was added dimethyl methylphosphonate (80.5 mmol, 8.73 mL). The light-yellow solution turned colorless and was stirred for an additional 45 min, during which time a white precipitate was formed. Next, 5-bromo-1-pentene (67 mmol, 10.0 g) was added, and after stirring at −45 °C for 30 min, the solution was allowed to warm to room temperature. The precipitate dissolved as the solution warmed, and the solution was stirred 1 additional h. Next, the clear, colorless solution was quenched with water, washed with brine, dried with $MgSO_4$ and filtered, and the solvent was removed to yield **5a** (crude yield ∼70%) which was purified by distillation (55 °C/0.05 Torr) to afford a colorless oil. ^{1}H NMR (400 MHz, C_6D_6): δ 5.63 (m, 1H), 4.93 (m, 2H), 3.38 (d, 6H, 11.2 Hz), 1.81 (q, 2H, 7.2 Hz), 1.50 (m, 4H), 1.19 (m, 2H); ^{13}C NMR (100 MHz, C_6D_6): δ 138.8, 115.3, 52.2 (d, 6.1 Hz), 34.1, 30.5 (d, 15.9 Hz), 26.4, 25.0, 22.9 (d, 4.9); ^{31}P NMR (162 MHz, C_6D_6): δ 34.9. HRMS (*m*/*z*): [M$^+$] calcd for $C_8H_{17}O_3P$, 192.0915; found, 192.0913. Anal. Calcd for $C_8H_{17}O_3P$: C, 49.99; H, 8.92. Found: C, 50.34; H, 8.89.

Hex-5-enylphosphine (5b). The phosphonate **5a** was reduced using $AlCl_2H$ in tetraglyme as described for **1b**, and product phosphine **5b** was vacuum-transferred away from the tetraglyme solution into a storage tube (cooled to −196 °C) containing activated 4 Å molecular sieves and C_6D_6. The final solution concentration was slightly less than 1 M by NMR, indicating an approximately 40% yield. ^{1}H NMR (400 MHz, C_6D_6): δ 5.68 (m, 1 H), 4.95 (m, 2H), 2.58 (d of t, 190 Hz, 7.2 Hz, 2H), 1.84 (q, 7.2 Hz, 2H), 1.21 (m, 6H); ^{13}C NMR (100 MHz, C_6D_6): δ 139.1, 115.1, 34.3, 33.3, (d, 3.1 Hz), 30.7 (d, 5.3 Hz), 14.5 (d, 8.3 Hz); ^{31}P NMR (162 MHz, C_6D_6): δ −137.2 (t, $^1J_{P-H}$ = 189.5 Hz). HRMS (*m*/*z*): [MH$^+$] calcd for $C_6H_{13}P$, 117.083; found, 117.083.

Synthesis of 1-Methylhex-5-enylphosphine (7). Diethyl-1-methylhex-5-enylphosphonate (7a). Phosphonate **7a** was prepared in the same manner as **3a**, using diethyl ethylphosphonate (14.02 g, 84.4 mmol), *n*-BuLi (1.6 M, 84.4 mmol, 52.3 mL), and 5-bromo-1-pentene (10.0 mL, 84.4 mmol). The resulting phosphonate was purified by distillation (62 °C/0.05 Torr) to afford a colorless oil in approximately 65% yield. ^{1}H NMR (400 MHz, C_6D_6): δ 5.57 (m, 1H), 4.93 (m, 2H), 3.90 (m, 4H), 1.90 (q, 6.6 Hz, 3H), 1.74 (m, 1H), 1.38 (m, 3H), 1.11 (d of d, 18.2 Hz, 7.0 Hz, 3H), 1.05 (t, 7.0 Hz, 6H); ^{13}C NMR (100 MHz, C_6D_6): δ 139.0, 115.2, 61.4 (t, 6.0 Hz), 34.5, 32.5, 31.2, 30.7 (d, 3.4 Hz), 27.6 (d, 12.5 Hz), 17.3 (d, 5.3 Hz), 14.3 (d, 4.9 Hz); ^{31}P NMR (121 MHz, C_6D_6): δ 35.2. HRMS (*m*/*z*): [M$^+$] calcd for $C_{11}H_{23}O_3P$, 234.1385; found, 234.1286. Anal. Calcd for $C_{11}H_{23}O_3P$: C, 56.39; H, 9.90. Found: C, 56.23; H, 9.92.

1-Methylhex-5-enylphosphine (7b). The phosphonate **7a** was reduced using $AlCl_2H$ in tetraglyme as described for **1b**, and product phosphine **7b** was vacuum-transferred away from the tetraglyme solution into a storage tube (cooled to −196 °C) containing activated 4 Å molecular sieves and C_6D_6. The final solution concentration was slightly less than 1 M by NMR, indicating an approximately 40% yield. ^{1}H NMR (400 MHz, C_6D_6): δ 5.7 (m, 1 H), 4.95−4.91 (m, 2H), 2.66 (d of t, 189 Hz, 7.5 Hz, 2H), 1.86 (q, 6.8 Hz, 2H), 1.56 (qu, 6.0 Hz, 1H), 1.26 (m, 4H), 0.98 (d of d, 12.4 Hz, 7.2 Hz, 3H); ^{13}C NMR (75 MHz, C_6D_6): δ 138.6, 114.6, 38.9 (d, 8.3 Hz), 34.0, 27.8 (d, 7.5 Hz), 23.3 (d, 7.9 Hz), 22.5 (d, 5.7 Hz); ^{31}P NMR (121 MHz, C_6D_6): δ −111.5 (t, $^1J_{P-H}$ = 188.6 Hz). HRMS (*m*/*z*): [MH$^+$] calcd for $C_7H_{15}P$, 131.098; found, 131.096.

Synthesis of 5-phenyl-4-pentynylphosphine (9). Diethyl-5-phenyl-4-pentynylphosphonate (9a). The reagent 5-phenyl-4-pentynyl-1-bromide was prepared as described previously.[12b] This bromide (3.71 g, 16.6 mmol) was reacted with neat $P(OEt)_3$ (3.13 mL, 18.3 mmol) at 150 °C overnight, and the resulting phosphonate was purified by distillation (135 °C/0.05 Torr) to afford **9a** as a colorless oil in approximately 70% yield. ^{1}H NMR (300 MHz, C_6D_6): δ 7.39 (m, 2H), 6.97 (m, 3H), 3.90 (m, 4H), 2.22 (t, 6.9 Hz, 2H), 1.80 (m, 4H), 1.02 (t, 6.9 Hz, 6H); ^{13}C NMR (75 MHz, C_6D_6): δ 132.3, 128.9, 128.2, 89.7, 82.5, 61.7 (d, 6.7 Hz), 26.6, 24.7, 22.9 (d, 4.9 Hz), 20.7 (d, 17.6 Hz), 16.9 (d, 5.4 Hz); ^{31}P NMR (121 MHz, C_6D_6): δ 31.7. HRMS (*m*/*z*): [M$^+$] calcd for $C_{15}H_{21}O_3P$, 280.1228; found, 280.1205. Anal. Calcd for $C_{15}H_{21}O_3P$: C, 64.26; H, 7.56. Found: C, 64.18; H, 7.66.5-phenyl-4-pentynylphosphine **(9b).** To a mixture of dichloroalane[24] [$AlCl_3$ (5.76 g, 40 mmol) and $LiAlH_4$ (0.53 g, 14 mmol)] in 50 mL of diethyl ether was added **9a** (2.0 g, 7.1 mmol), and the gray solution was stirred under nitrogen overnight. The reaction was then quenched with deoxygenated water at 0 °C, and the upper organic layer was separated via cannula, dried over $MgSO_4$ and filtered, and solvent was removed in vacuo to yield a light-yellow oil. Purification by distillation (90 °C/0.07 Torr) afforded the primary phosphine **9b** as a colorless oil (0.81 g, 65% yield), which was stored in an airtight storage tube as a solution in C_6D_6 over activated 4 A molecular sieves. ^{1}H NMR (300 MHz, C_6D_6): δ 7.44 (m, 2H), 6.99 (m, 3H), 2.53 (d of t, 191 Hz, 7.5 Hz, 2H), 2.13 (t, 6.9 Hz, 2H), 1.46 (qu, 7.2 Hz, 2H), 1.26 (m, 2H); ^{13}C NMR (75 MHz, C_6D_6): 132.3, 128.9, 128.2, 125.0, 90.1, 82.2, 32.7 (d, 3.0 Hz), 20.9 (d, 5.5 Hz), 13.7 (d, 9.2 Hz); ^{31}P NMR (121 MHz, C_6D_6): δ −138.2 (t, $^1J_{P-H}$ = 190 Hz). HRMS (*m*/*z*): [M$^+$] calcd for $C_{11}H_{13}P$, 176.0756; found, 176.0781. Anal. Calcd for $C_{11}H_{13}P$: C, 74.98; H, 7.44. Found: C, 74.58; H, 7.24.

Synthesis of 6-Phenyl-5-hexynylphosphine (11). Diethyl-6-phenyl-5-hexynylphosphonate (11a). The reagent 6-phenyl-5-hexynyl-1-bromide was prepared as described previously.[12b] This bromide (10.63 g, 44.9 mmol) was reacted with neat $P(OEt)_3$ (9.2 mL, 53.8 mmol) at 150 °C overnight, and the resulting phosphonate **11a** purified by distillation (160 °C/0.05 Torr) to afford **11a** as a colorless oil (9.0 g, 68% yield). ^{1}H NMR (300 MHz, C_6D_6): δ 7.49 (m, 2H), 6.99 (m, 3H). 3.93 (m, 4H), 2.13 (t, 7.0 Hz, 2H), 1.72 (m, 2H), 1.50 (m, 4H), 1.04 (t, 6.9 Hz, 6H); ^{13}C NMR (75 MHz, C_6D_6): δ 132.2, 128.9, 128.1, 125.1, 90.3, 82.1, 61.4 (d, 6.5), 29.9 (d, 15.5), 27.1, 25.2, 22.6 (d, 5.0), 19.5, 16.9 (d, 5.6); ^{31}P NMR (121 MHz, C_6D_6): δ 32.1. HRMS (*m*/*z*): [M$^+$] calcd for $C_{16}H_{23}O_3P$, 294.1385; found, 294.1347.

6-Phenyl-5-hexynylphosphine (11b). The phosphonate **11a** was reduced using $AlCl_2H$ in diethyl ether as described for **9b**. Purification by bulb-to-bulb distillation (130 °C/0.05 Torr) gave the primary phosphine **11b** in 55% yield (0.71 g), which was stored in an airtight storage tube as a solution in C_6D_6 over activated 4 A molecular sieves. ^{1}H NMR (300 MHz, C_6D_6): δ 7.49 (m, 2H), 6.99 (m, 3H), 2.56 (d of t, 190 Hz, 7.5 Hz, 2H), 2.12 (t, 6.6 Hz, 2H), 1.35 (m, 4H), 1.10 (m, 2H); ^{13}C NMR (75 MHz, C_6D_6): 132.3, 128.9, 128.1, 125.1, 90.6, 82.0, 32.8 (d, 3.2 Hz), 30.2 (d, 5.5 Hz), 19.6, 13.8 (d, 8.6 Hz); ^{31}P NMR (121 MHz, C_6D_6): δ −137.3 (t, $^1J_{P-H}$ = 190 Hz). HRMS (*m*/*z*): [M$^+$] calcd for $C_{12}H_{15}P$, 190.0912; found, 190.0917.

Synthesis of Pent-4-enylphenylphosphine (13). Pent-4-enyldiphenylphosphine (13a). A solution of 50 mL of $KPPh_2$ (0.5 M in THF) and 50 mL of THF was stirred under nitrogen. Next, 5-bromo-1-pentene (3.0 mL, 35 mmol) was added dropwise, and the resulting viscous orange solution was stirred for 90 min. The THF was then removed in vacuo, and 20 mL of pentane was added to the orange residue. Next, deoxygenated water was added via cannula, and the resulting clear, colorless organic layer was decanted via cannula, dried over $MgSO_4$ and filtered via cannula, and then the solvent was removed in vacuo to yield a light-yellow oil. This material was distilled (80 °C/0.05 Torr) to give a pure light-yellow oil (7.0 g) in 79% yield. NMR spectra agree with the literature data for pent-4-enyldiphenylphosphine.[25] ^{1}H NMR (300 MHz, C_6D_6): δ 7.42 (m, 4H), 7.06 (m, 6H), 5.6 (m, 1 H), 4.97−4.91 (m, 2H), 2.01 (q, 7.2 Hz, 2H), 1.91 (m, 2H), 1.51 (qu, 8.1 Hz, 2H); ^{13}C NMR (75 MHz, C_6D_6): δ 138.6, 133.6, 133.3, 129.1, 129.0, 115.6, 35.7 (d, 13.4 Hz), 28.2 (d, 12.1 Hz), 26.0 (d, 17.0 Hz); ^{31}P NMR (121 MHz, C_6D_6): δ −15.6. HRMS (*m*/*z*): [M$^+$] calcd for $C_{17}H_{18}P$, 253.1147; found, 253.1114. Anal. Calcd for $C_{17}H_{19}P$: C, 80.29; H, 7.53. Found: C, 80.31; H, 7.48.

Pent-4-enylphenylphosphine (13b). To 40 mL of $NH_{3(l)}$ was added 0.27 g (11.8 mmol) of Na spheres, and the resulting blue solution was stirred at −78 °C under nitrogen for 1.0 h. Next, 1.50 g (5.9 mmol) **13a** was added, and the reaction mixture was stirred at −50 °C for ∼3 h until it became golden yellow. Solid NH_4Cl (0.63 g, 54 mmol) was next added under a nitrogen flush, and the colorless reaction mixture was allowed to stir and warm to room temperature (with ammonia

(25) Sigl, M.; Schier, A.; Schmidbaur, H. *Chem. Ber.* **1997**, *130*, 951−954.

boiling off) overnight. Diethyl ether was then added, the resulting solution decanted via cannula filtration, solvent removed in vacuo, and the resulting oil purified by distillation (70 °C/0.05 Torr) to afford 0.75 g of a colorless oil (60% yield), which was stored in an airtight storage tube as a solution in C_6D_6 over activated 4 A molecular sieves at low temperature with exclusion of light. ^{1}H NMR (300 MHz, C_6D_6): δ 7.36 (m, 2H), 7.06 (m, 3H), 5.59 (m, 1H), 4.93 (m, 2H), 4.08 (d of t, 205 Hz, 7.2 Hz, 1H), 1.89 (q, 7.0 Hz, 2H), 1.53 (m, 2H), 1.42 (m, 2H); ^{13}C NMR (75 MHz, C_6D_6): δ 138.6, 134.3 (d, 15.8 Hz), 129.0, 128.9, 128.6, 115.5, 35.5 (d, 8.6 Hz), 28.1 (d, 7.9 Hz), 23.4 (d, 11.5 Hz); ^{31}P NMR (121 MHz, C_6D_6): δ −51.3 (d, $^1J_{P-H}$ = 202 Hz). HRMS (*m*/*z*): [M$^+$] calcd for $C_{11}H_{15}P$, 178.0912; found, 178.0909.

Synthesis of 1-Methylpent-4-enylphenylphosphine (15). 1-Methylpent-4-enyldiphenylphosphine (15a). Using the published procedure,[26] 5-hexen-2-one was reduced to the corresponding alcohol and then converted to 5-hexene-2-methanesulfonate. Halogenation of the alcohol did not provide acceptable yields for the next step of the synthesis. Therefore, the mesylate (2.48 g, 14 mmol) was stirred under nitrogen in 50 mL of THF, and $KPPh_2$ (0.5 M in THF) was added (28 mL, 14 mmol) via syringe. The resulting viscous orange/red solution was stirred for an additional 90 min, and then solvent was removed under vacuum. Pentane was added to the orange residue, and then deoxygenated water was added. The colorless organic layer was separated via cannula, dried over $MgSO_4$ and filtered, and the solvent was removed to yield a light-yellow oil which was of sufficient purity for subsequent syntheses (2.3 g, 61% yield) or was distilled (90 °C/0.1 Torr) to afford **15a** as a colorless oil. ^{1}H NMR (300 MHz, C_6D_6): δ 7.53 (m, 4H), 7.06 (m, 6H), 5.65 (m, 1H), 4.93 (m, 2H), 2.25 (m, 1H), 2.18 (m, 1H), 1.95 (m, 1H), 1.65 (m, 1H), 1.35 (m, 1H), 1.00 (d of d, 14.4 Hz, 6.9 Hz, 3H); ^{13}C NMR (75 MHz, C_6D_6): δ 138.9, 134.7, 134.4, 134.3, 134.1, 129.2, 129.1, 129.0, 129.0, 128.9, 128.9, 115.4, 33.3 (d, 18.2 Hz), 32.2 (d, 12.1 Hz), 29.9 (d, 10.9 Hz), 16.5 (d, 15.8 Hz); ^{31}P NMR (121 MHz, C_6D_6): δ −0.70. HRMS (*m*/*z*): [M$^+$] calcd for $C_{18}H_{21}P$, 268.1381; found, 268.1341 (loss of 1 H, [M − 1$^+$] calcd for $C_{18}H_{20}P$, 267.1301; found, 267.1301).

1-Methylpent-4-enylphenylphosphine (15b). To a stirring suspension of Li powder (0.37 g, 53.3 mmol) in THF (50 mL) under argon was added **15a** (2.8 g, 10.4 mmol). The gray solution gradually turned orange, and stirring was continued ∼2.5 h. Under an Ar flush, ca. 3 g of NH_4Cl was then added, and the color changed back to gray. The THF was then removed under vacuum, and the residue was dissolved in 20 mL of pentane. The liquid was separated via cannula filtration, and pentane was removed in vacuo to yield a light-yellow oil. Distillation (40 °C/0.06 Torr) using a Vigreux column to ensure separation of the byproduct Ph_2PH yielded 0.40 g (20%) of **15b**, a colorless oil, which was stored in an airtight storage tube as a solution in C_6D_6 over activated 4 A molecular sieves at low temperature with exclusion of light. Both *cis* and *trans* forms of **15b** are present in equal amounts as assayed by ^{1}H NMR, and the ^{13}C NMR and ^{31}P NMR exhibit twice as many signals as would be expected for a single isomer. ^{1}H NMR (300 MHz, C_6D_6): δ 7.39 (m, 2H), 7.06 (m, 3H), 5.65 (m, 1H), 4.93 (m, 2H), [4.5 (d of d, 206 Hz, 5.4 Hz) and 3.94 (d of d, 206 Hz, 6.3 Hz) together 1H], 2.05 (m, 3H), 1.51 (m, 1H), 1.30 (m, 1H), [0.98 (q, 6.9 Hz) and 0.92 (q, 7.2 Hz) together 3H]; ^{13}C NMR (75 MHz, C_6D_6): δ 138.8, 135.7, 135.5, 135.3, 135.1, 128.9, 128.9, 115.3, 35.5 (d, 10.4 Hz), 35.3 (d, 15.2 Hz), 32.7 (d, 3.6 Hz), 32.6 (d, 6.7 Hz)], 29.8 (d, 10.9 Hz), 29.3 (d, 9.8 Hz) 20.1 (d, 5.4 Hz) 19.0 (d, 15.2 Hz); ^{31}P NMR (121 MHz, C_6D_6): δ −27.4, −32.2 (d, $^1J_{P-H}$ = 206 and 205 Hz, respectively). HRMS (*m*/*z*): [M$^+$] calcd for $C_{12}H_{17}P$, 192.1068; found, 192.10718.

Synthesis of 2,2-Dimethylpent-4-enylphenylphosphine (17). 2,2-Dimethylpent-4-enyldiphenylphosphine (17a). Using the published procedure, 2,2-dimethyl-4-pentenal was prepared.[27] This product was subsequently reduced with $LiAlH_4$ to 2,2-dimethyl-pent-4-en-1-ol, and final traces of *p*-cymene (the solvent in preparation of the aldehyde) were removed via flash chromatography. This alcohol was then converted to the mesylate, and the mesylate was subjected to reaction with $KPPh_2$ to form **17a** as described above for **15a** (71% crude yield), and purified by distillation (120 °C/0.07 Torr) to afford **17a** as a colorless oil. ^{1}H NMR (300 MHz, C_6D_6): δ 7.48 (m, 4H), 7.05 (m, 6H), 5.59 (m, 1H), 4.93 (m, 2H), 2.13 (m, 4H), 0.97 (s, 6H); ^{13}C NMR (75 MHz, C_6D_6): δ 141.3 (d, 13.6 Hz), 135.9, 133.9, 133.6, 129.1, 129.0, 128.8, 118.0, 48.5 (d, 8.5 Hz), 43.3 (d, 17.5 Hz), 34.8 (d, 14.6 Hz), 29.1 (d, 9.5 Hz); ^{31}P NMR (121 MHz, C_6D_6): δ −23.8. HRMS (*m*/*z*): [M$^+$] calcd for $C_{19}H_{23}P$, 282.1536; found, 282.1537.

2,2-Dimethylpent-4-enylphenylphosphine (17b). This product was prepared from **17a** in a manner analogous to preparation of **15b** from **15a**. Purification by bulb-to-bulb distillation (110 °C/0.10 Torr) yielded a clear colorless oil (0.67 g) in 46% yield that was stored in an airtight storage tube as a solution in C_6D_6 over activated 4 A molecular sieves at low temperature with exclusion of light. ^{1}H NMR (300 MHz, C_6D_6): δ 7.43 (m, 2H), 7.06 (m, 3H), 5.71 (m, 1H), 5.02 (m, 2H), 4.08 (d of d of d, 206 Hz, 9.5 Hz, 7.8 Hz, 1H), 2.05 (m, 3H), 1.46 (m, 1H), 0.93 (s, 6H); ^{13}C NMR (75 MHz, C_6D_6): 137.3, 135.8, 134.6, 129.1, 129.0, 128.6, 127.7, 117.9, 47.9 (d, 7.5 Hz), 38.0 (d, 13.5 Hz), 34.3 (d, 9 Hz), 28.5 (d, 8.6 Hz); ^{31}P NMR (121 MHz, C_6D_6): δ −67.2 (d, $^1J_{P-H}$ = 205 Hz). HRMS (*m*/*z*): [M$^+$] calcd for $C_{13}H_{19}P$, 206.1224; found, 206.1229.

Typical NMR-Scale Catalytic Reactions. In the glovebox, the organolanthanide precatalyst (2−3 mg) was weighed into an NMR tube equipped with a Teflon valve, and C_6D_6 was added (ca. 500 μL). On the high-vacuum line, the tube was evacuated while the benzene solution was frozen at −78 °C, and then the substrate (ca. 1.0 M in C_6D_6, 0.2−0.3 mL, 30−150-fold molar excess) was added either via syringe under an Ar flush or by vacuum-transfer (depending on substrate volatility). The tube was evacuated and backfilled with Ar three times while frozen at −78 °C, and then the tube was sealed, thawed, brought to the desired temperature, and the ensuing reaction was monitored by ^{1}H and ^{31}P NMR.

Synthesis of 2-Methylphospholane (2). The precatalyst and substrate **1** were combined as described above and sealed in an NMR tube; the ensuing cyclization was monitored by ^{1}H and ^{31}P NMR. The cyclization proceeded until all of the starting material had been consumed as judged by NMR and the desired products composed 91% of the final reaction mixture.[28] The ^{1}H assignment (similar to that previously reported)[21a] is ^{1}H NMR (500 MHz, C_6D_6): δ 3.01 (d of t, 183.5 Hz, 8.0 Hz, 1H, minor isomer), 2.46 (d of m, 191 Hz, major isomer), 2.24 (m, 1H, minor isomer), 1.71 (m, 6H), 1.39 (m, 4H), 1.09 (d of d, 10.7 Hz, 6.2 Hz, 3H), 1.07 (m, 2H), 1.02 (d of d, 18.5 Hz, 7.5 Hz, 3H); ^{13}C NMR (75 MHz, C_6D_6): δ 40.5 (d, 6.1 Hz), 39.5 (d, 3.8 Hz), 32.7 (d, 8.4 Hz), 30.6 (d, 5.3 Hz), 29.5 (d, 4.6 Hz), 28.8 (d, 5.3 Hz), 21.2 (d, 31.0 Hz), 20.53 (d, 10.6 Hz), 20.45 (d, 9.9 Hz), 19.9 (s); ^{31}P NMR (121 MHz, C_6D_6): δ −44.7 (d, $^1J_{P-H}$ = 180.9 Hz, 61%), −54.4 (d, $^1J_{P-H}$ = 181.0 Hz, 30%). HRMS (*m*/*z*): [MH$^+$] calcd for $C_5H_{12}P$, 103.0671; found, 103.0683.

The major and minor isomer features in the ^{1}H NMR were correlated with the corresponding isomers in the ^{31}P NMR using HMQC spectroscopy. The structure of **2** was established through 2D ^{1}H−^{1}H NOESY spectroscopy. The major isomer P−H proton (^{1}H NMR: δ 2.46 (d of m, $^1J_{P-H}$ =191 Hz); ^{31}P NMR: δ −44.7) exhibited a cross-peak with the exo methyl group at δ 1.09 (d of d, 10.7 Hz, 6.2 Hz, 3H) showing that the proton and methyl group are proximate, therefore assigning the major ^{31}P NMR resonance at δ −44.7 ppm to isomer **2b.** In addition, another study[29a] assigns the same configuration based on J_{P-C} coupling constant arguments, and another[29b] assigns the same configuration based on J_{P-C-CH_3} coupling constants.

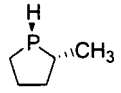

2a, *trans*

^{31}P δ -54.4

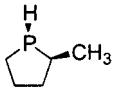

2b, *cis*

^{31}P δ -44.7

Synthesis of 2,5-Dimethylphospholane (4). The precatalyst and substrate were combined as described above and sealed in an NMR

(26) Becker, D.; Haddad, N. *Tetrahedron* **1993**, *49*, 947−964.
(27) Semmelhack, M. F., Ed. *Org. Synth.* **1984**, *62*, 125−133.
(28) For compound **2**, 22 proton signals and 10 carbon signals are assigned instead of 11 and 5, respectively, due to the presence of both product diastereomers in an approximately 2:1 ratio.

tube; the ensuing cyclization was monitored by ^{1}H and ^{31}P NMR. The cyclization proceeded until all of the starting material had been consumed as judged by NMR. The ratio of the configurations of the various products varied with catalyst (see text). On the basis of comparisons between the predominantly *cis* and predominantly *trans* spectra, assignments for the *cis* and *trans* products can be made. *trans*-Isomer:[30] ^{1}H NMR (300 MHz, C_6D_6): δ 2.78 (d of t, 180 Hz, 9.3 Hz, 1H), 2.35 (m, 1H), 1.86 (m, 3H), 1.63 (m, 1H), 1.28 (m, 1H), 1.08 (d of d, 10.8 Hz, 6.6 Hz, 6H); ^{13}C NMR (125 MHz, C_6D_6): δ 41.09 (d, 5.0 Hz), 39.01, 32.81 (7.5 Hz), 29.61, 22.01 (d, 30.5 Hz), ^{31}P NMR (121 MHz, C_6D_6): δ −28.3 (d, 173 Hz). *cis*-Isomer: ^{1}H NMR (400 MHz, C_6D_6): δ 2.26 (d of m, 191 Hz, 1H), 1.88 (m, 2H), 1.65 (m, 2H), 1.28 (m, 2H), 0.97 (d of d, 16.8 Hz, 7.6 Hz, 6H); ^{13}C NMR (125 MHz, C_6D_6): δ 38.50 (d, 5.0 Hz), 33.07 (d, 9.0 Hz), 21.18; ^{31}P NMR (121 MHz, C_6D_6): δ −13.4 (d, $^1J_{P-H}$ = 179 Hz). HRMS (*m*/*z*): [MH$^+$] calcd for $C_6H_{14}P$, 117.0833; found, 117.0844.

Synthesis of 2-Methylphosphorinane (6). The precatalyst and substrate were combined as described above and sealed in an NMR tube; the ensuing cyclization was monitored by ^{1}H and ^{31}P NMR. The cyclization proceeded until all of the starting material had been consumed as judged by NMR and the major product composed 89% of the final reaction mixture. ^{1}H NMR (400 MHz, C_6D_6): δ 2.74 (d of t, 185.2 Hz, 12.0 Hz, 1H), 1.80 (m, 2H), 1.61 (m, 1H), 1.48 (m, 2H), 1.11 (m, 4H), 1.00 (d of d, 16.8 Hz, 6.8 Hz, 3H); ^{13}C NMR (100 MHz, C_6D_6): δ 39.7 (d, 5.7 Hz), 29.1 (d, 3.0 Hz), 28.7, 26.8 (d, 7.2 Hz), 22.4 (d, 14.1 Hz), 20.0 (d, 11.4 Hz); ^{31}P NMR (162 MHz, C_6D_6): δ −44.6 (d, 183 Hz). (About 10% of the minor isomer is produced as assayed by ^{31}P NMR: δ −62.1 (d, 194 Hz.) HRMS (*m*/*z*): [M$^+$] calcd for $C_6H_{13}P$, 116.0755; found, 116.0754.

Synthesis of 2,6-Dimethylphosphorinane (8). The precatalyst and substrate were combined as described above and sealed in an NMR tube; the ensuing cyclization was monitored by ^{1}H and ^{31}P NMR. The cyclization proceeded until all of the starting material had been consumed as judged by NMR and the major product composed 86% of the final reaction mixture. ^{1}H NMR (400 MHz, C_6D_6): δ 2.74 (d of t, 185.2 Hz, 12.0 Hz, 1H), 1.80 (m, 2H), 1.68 (m, 2H), 1.23 (m, 2H), 1.02 (d of d, 16.4 Hz, 7.2 Hz, 6H), 0.88 (m, 2H); ^{13}C NMR (125 MHz, C_6D_6): δ 38.6 (d, 5.5 Hz), 28.6 (s), 27.2 (d, 8.5 Hz), 21.7 (d, 13.5 Hz); ^{31}P NMR (162 MHz, C_6D_6): δ −25.6 (d, $^1J_{P-H}$ = 186 Hz). [There are two minor isomers present in the ^{31}P spectra: δ −35.6 (d, 182.5 Hz, ∼2%) and δ −47.5 (d, 180 Hz, ∼2%).] HRMS (*m*/*z*): [MH$^+$] calcd for $C_7H_{16}P$, 131.098; found, 131.095.

Synthesis of 2-(1-Phenyl-2-ethenyl)phospholane (10). The precatalyst and substrate were combined as described above and sealed in an NMR tube, and the ensuing cyclization was monitored by ^{1}H and ^{31}P NMR. The cyclization proceeded until all of the starting material had been consumed as judged by NMR. The product formed was stable for several hours but decomposed slowly to many uncharacterized products with mass spectrometric molecular weights corresponding roughly to dimers. ^{1}H NMR (300 MHz, C_6D_6): δ 7.17 (m, 3H), 7.04 (m, 3H), 3.78 (d of m, 180 Hz, 1H), 2.52 (m, 1H), 2.14 (m, 1H), 1.81 (m, 1H), 1.62 (m, 1H), 1.44 (m, 1H), 1.23 (m, 1H); ^{13}C NMR (75 MHz, C_6D_6): δ 133.5 (d, 34.6 Hz), 132.2, 129.2, 128.9, 127.4, 34.5 (d, 1.9 Hz), 33.1 (d, 6.1 Hz), 21.3 (d, 4.9 Hz); ^{31}P NMR (121 MHz, C_6D_6): δ −55.1 (d, $^1J_{P-H}$ = 181 Hz). HRMS (*m*/*z*): [M$^+$] calcd for $C_{11}H_{13}P$, 176.0754; found, 176.0755.

Synthesis of 2-(2-Phenyl-1-ethenyl)phosphorinane (12). The precatalyst and substrate were combined as described above and sealed in an NMR tube, and the ensuing cyclization was monitored by ^{1}H and ^{31}P NMR. The cyclization proceeded until all of the starting material had been consumed as judged by NMR. The product formed was stable for several hours, but decomposed slowly to many uncharacterized products with mass spectrometric molecular weights corresponding roughly to dimers. ^{1}H NMR (300 MHz, C_6D_6): δ 7.17 (m, 3H), 7.04 (m, 3H), 3.84 (d of d of m, 191 Hz, 12.3 Hz, 1H) 3.13 (d of quart, 12 Hz, 3.9 Hz, 1H), 2.08 (m, 1H), 2.01 (m, 1H), 1.82 (m, 1H), 1.55 (m, 2H), 1.41 (m, 1H), 1.13 (m, 1H); ^{13}C NMR (75 MHz, C_6D_6): δ 138.8 (d, 49.6 Hz), 133.3, 129.6, 128.8, 127.5, 33.5 (d, 5.0 Hz), 29.6 (d, 2.0 Hz), 29.3, 21.8 (d, 8.5 Hz); ^{31}P NMR (121 MHz, C_6D_6): δ −53.1 (d, $^1J_{P-H}$ = 191.5 Hz).

Synthesis of 2-Methyl-1-phenylphospholane (14). The precatalyst and substrate were combined as described above and sealed in an NMR tube, and the ensuing cyclization was monitored by ^{1}H and ^{31}P NMR. The cyclization proceeded until all of the starting material had been consumed as judged by NMR and the desired product composed ∼74.5% of the final reaction mixture.[31] ^{1}H NMR (300 MHz, C_6D_6): δ 7.32 (m, 2H), 7.11 (m, 3H), 2.17 (m, 1H), 1.82 (m, 3H), 1.67 (m, 1H), 1.55 (m, 1H), 1.23 (d of d, 18.9 Hz, 7.5 Hz, 3H), 1.14 (m, 1H); ^{13}C NMR (75 MHz, C_6D_6): δ 131.3 (d, 16 Hz), 129.0, 128.9, 127.9, 38.7 (d, 11 Hz, CH), 37.7 (s, CH_2), 28.2 (d, 3.7 Hz, CH_2), 27.1 (d, 14.0 Hz, CH_2), 20.7 (d, 32.8 Hz, CH_3); ^{31}P NMR (121 MHz, C_6D_6): δ 1.7 (major), −6.3 (minor). HRMS (*m*/*z*): [M$^+$] calcd for $C_{11}H_{15}P$, 178.0911; found, 178.0926.

Synthesis of 2,5-Dimethyl-1-phenylphospholane (16). The precatalyst and substrate were combined as described above and sealed in an NMR tube, and the ensuing was cyclization monitored by ^{1}H and ^{31}P NMR. The cyclization proceeded until all of the starting material had been consumed as judged by NMR and the desired product composed ∼70% of the final reaction mixture. NMR showed conversion to two products in approximately equal amounts, with twice as many signals observed as would be expected for a single isomer.[32] ^{1}H NMR (500 MHz, C_6D_6): δ 7.54 (m, 1H), 7.40 (m, 1H), 7.13 (m, 3H), 2.52 (m, 1H), 2.20 (m, 1H), 2.05 (m, 2H), 1.76 (m, 2H), 1.56 (m, 2H), 1.41 (m, 1H), 1.35 (m, 1H), 1.26 (d of d, 19.0 Hz, 7.4 Hz, 6H), 1.25 (d of d, 18.5 Hz, 7.5 Hz, 3H), 1.12 (m, 2H), 0.76 (d of d, 10.6 Hz, 7.0 Hz, 3H); ^{13}C NMR (75 MHz, C_6D_6): δ 135.0 (d, 19.0 Hz), 131.7 (d, 16.0 Hz), 129.2, 128.9, 128.9, 128.8, 128.5, 128.1, 38.4 (d, 10.1 Hz), 37.5 (s), 36.5 (s), 36.0 (d, 12.5 Hz), 35.6 (d, 10.0 Hz), 21.6 (d, 35.6 Hz), 21.4 (d, 33.1 Hz), 15.7 (s); ^{31}P NMR (121 MHz, C_6D_6): δ 19.5, 10.5. HRMS (*m*/*z*): [M$^+$] calcd for $C_{12}H_{17}P$, 192.1068; found, 192.1067.

Synthesis of 4,4-Dimethyl-2-methyl-1-phenylphospholane (18). The precatalyst and substrate were combined as described above and sealed in an NMR tube, and the ensuing cyclization was monitored by ^{1}H and ^{31}P NMR. The cyclization proceeded until all of the starting material had been consumed as judged by NMR and the desired product composed 70−90% of the final reaction mixture. NMR showed conversion to two products in approximately equal amounts, with twice as many signals observed as would be expected for a single isomer.[33] ^{1}H NMR (500 MHz, C_6D_6): δ 7.53 (t, 3.9 Hz, 1H), 7.32 (t, 4.5 Hz, 1H), 7.13 (m, 3H), 2.41 (m, 2H), 1.98 (m, 2H), 1.90 (m, 2H), 1.78 (m, 2H), 1.55 (m, 1H), 1.47 (m, 1H), 1.37 (d of d, 17.5 Hz, 6.0 Hz, 3H), 1.12 (s, 3H), 0.98 (s, 3H), 0.92 (s, 3H), 0.74 (d of d, 6.3 Hz, 4.2 Hz, 3H), 0.66 (s, 3H); ^{13}C NMR (75 MHz, C_6D_6): δ 134.8 (d, 20 Hz), 129.7, 129.6, 129.1, 128.8, 128.6, 128.5, 127.3, 52.4 (d, 4.6), 51.3 (d, 3.8), 42.9 (s), 41.7 (s), 41.0 (d, 13.6), 39.9 (d, 13.6), 37.5 (d, 9.8), 33.4 (d, 11.4), 31.3 (d, 4.6), 31.1 (s), 30.2 (s), 28.8 (s), 21.2 (d, 32.6), 15.9 (s); ^{31}P NMR (121 MHz, C_6D_6): δ 3.7, 1.3. HRMS (*m*/*z*): [M$^+$] calcd for $C_{13}H_{19}P$, 206.1222; found, 206.1221.

Synthesis of *n*-Pentylphosphine (19). Diethyl *n*-Pentylphosphonate (19a). The reagent 1-bromopentane (16.4 mL, 132 mmol) was reacted with $P(OEt)_3$ (25.0 mL, 146 mmol) at 150 °C overnight, and

(29) (a) Langhans, K. P.; Stelzer, O. *Z. Naturforsch.* **1990**, *45b*, 203−211. (b) Couret, C.; Escudie, J.; Thaoubane, S. A. *Phosphorus Sulfur* **1984**, *20*, 81−86.

(30) Phospholane **4a** (*trans* isomer) was prepared recently by another method: Burk, M. J.; Pizzano, A.; Martín, J. A.; Liable-Sands, L. M.; Rheingold, A. L. *Organometallics* **2000**, *19*, 250−260.

(31) Product **14** was obtained as a single isomer, and the ^{1}H and ^{13}C NMR reported here are for that single isomer. Formation of the six-membered ring byproduct was sufficiently suppressed to allow complete assignment of the product spectra.

(32) Final assignments of the ^{1}H and ^{13}C NMR spectra were made after subtracting peaks from the endocyclic six-membered ring (∼30% of the product mixture). For compound **16**, 24 nonphenyl ^{1}H signals and 8 ^{13}C signals are observed rather than 12 and 6, respectively, due to the presence of both product diastereomers in equal amounts. One set of signals corresponds to the spectra reported for the *trans* isomer synthesized by an alternative route (^{13}C spectra differ slightly): Burk, M. J.; Feaster, J. E.; Harlow, R. L. *Tetrahedron: Asymmetry* **1991**, *2(7)*, 569−592.

(33) Final assignments of the ^{1}H and ^{13}C NMR spectra were made after subtracting peaks from the endocyclic six-membered ring (∼5−30% of the product mixture). For compound **18**, 28 nonphenyl ^{1}H signals and 14 ^{13}C signals are observed rather than of 14 and 7, respectively, due to the presence of both product diastereomers in equal amounts.

the resulting phosphonate was purified twice by distillation (110 °C /8 Torr) to yield a colorless oil in approximately 80% yield. NMR spectra agree with the literature data.[34,35] ^{1}H NMR (400 MHz, C_6D_6): δ 3.94 (m, 4H), 1.57 (m, 4H), 1.13 (m, 4H), 1.06 (t, 6.8 Hz, 6H), 0.77 (t, 6.6 Hz, 3H); ^{13}C NMR (100 MHz, C_6D_6): δ 61.5 (d, 6.1 Hz), 33.6 (d, 16.0 Hz), 27.7, 26.3, 23.3 (d, 5.3 Hz), 23.1, 17.3 (d, 5.3 Hz), 14.6; ^{31}P NMR (162 MHz, C_6D_6): δ 32.7.

***n*-Pentylphosphine (19b).** Phosphonate **19a** was reduced using $AlCl_2H$ in tetraglyme as described for **1b**, and the phosphine **19b** was vacuum-transferred away from the tetraglyme solution into a storage tube (cooled to −78 °C) containing activated 4 A molecular sieves and C_7D_8. Final solution concentration was about 1 M by NMR, indicating an approximately 50% yield. ^{1}H NMR (400 MHz, C_7D_8): δ 2.58 (d of t, 189 Hz, 7.2 Hz, 2H), 1.28 (t, 6.8 Hz, 2H), 1.18 (m, 2H), 1.14 (m, 4H), 0.82 (t, 6.8 Hz, 3H); ^{13}C NMR (100 MHz, C_7D_8): δ 33.9 (d, 5.7 Hz), 33.8 (d, 3.8 Hz), 23.4, 14.9, 14.7 (d, 8.0 Hz); ^{31}P NMR (162 MHz, C_7D_8): δ −137.1 (t of m, 190 Hz).

Synthesis of Bis[(bispentamethylcyclopentadienyl)(μ-phenylphosphino)yttrium)] [Cp′$_2$YP(H)Ph]$_2$ (20). First, hydride precatalyst (Cp′$_2$YH)$_2$ was generated by stirring 165 mg of Cp′$_2$Y(CHTMS)$_2$ in 10 mL of toluene under an H_2 atmosphere overnight. Then an approximately 10-fold molar excess of $PhPH_2$ in benzene was added via syringe under an Ar flush to the red organoyttrium solution. The mixture turned orange and was stirred for 1.0 h, and then all volatiles were removed in vacuo. Toluene was next condensed onto the residue, the yellow mixture was stirred for 1.0 h, and then the toluene was removed in vacuo. This dissolution/evaporation process was repeated twice to ensure removal of all CH_2TMS_2. The resulting solid material proved to be only slightly soluble in pentane, even at reflux, and slow diffusion of pentane into toluene at various temperatures did not lead to the formation of crystalline material. Instead, the material was dissolved in toluene, filtered, and concentrated under vacuum until solid material began to precipitate from solution. At this point, the mixture was heated to 60 °C until a clear solution was obtained, and a color change from yellow to red was observed. The mixture was allowed to cool slowly to room temperature, and small colorless crystals were collected by decantation to obtain **20** in a very low overall yield. ^{1}H NMR (500 MHz, C_7D_8): δ 7.42 (s, 2H), 7.04 (m, 8H), (δ 3.46, J_1 = 129 Hz, J_2 = 76 Hz, 2H), 2.12 (s, 60H); ^{13}C NMR (125 MHz, C_7D_8): δ 138.6, 134.2, 126.4, 120.2, 13.5; ^{31}P NMR (202 MHz, C_7D_8): δ −107 (br).

X-ray Crystallographic Study of [Cp′$_2$YP(H)Ph]$_2$ (20). A suitable crystal of **20** was mounted using oil (Infineum V8512) on a glass fiber and mounted on a Bruker SMART-1000 CCD diffractometer. Crystal data collection parameters are listed in Table 1. Lattice parameters were determined from three sets of 20 frames and refined with all data. Cell reduction calculations on all data showed **20** to crystallize in the tetragonal space group $P4_2/m$.[36] Intensity data were corrected for Lorentz, polarization, and anomalous dispersion effects.[36] A numerical absorption correction was also applied with minimum and maximum transmission factors of 0.7376 and 0.8132, respectively. The structure was solved using direct methods.[37] The final cycles of full-matrix least-squares refinement were based on 3033 observed reflections ($I > 3.00\sigma(I)$) and 124 variable parameters, and converged (largest parameter shifts were 0.02 times the esd) with unweighted and weighted agreement factors of $R = 0.067$, $R_w^2 = 0.138$. Hydrogen atoms attached to carbon atoms were given idealized positions. The hydrogen atoms on the phosphorus centers could not be located. The Cp′ rings showed some disorder and therefore were not refined anisotropically, and the hydrogen atoms were not included. The largest peak in the final difference map (1.07 e$^-$/Å^3) was located near yttrium.

Kinetic Studies of Hydrophosphination/Cyclization. In a typical experiment, an NMR sample was prepared as described above (see Typical NMR-Scale Catalytic Reactions) but kept frozen at −78 °C until kinetic measurements were begun. Before the experiment, the NMR probe was equilibrated to the desired temperature and checked with a methanol or ethylene glycol temperature calibrant. The sample was then warmed quickly and inserted into the probe. Data were acquired using four scans per time interval, with a long pulse delay (8 s) to avoid signal saturation. Reactions were monitored by measuring the olefinic (for phosphinoalkenes) or P−H (for phosphinoalkynes) peaks versus the EH(*TMS*)$_2$ peak generated when catalytic turnover is initiated, and were monitored over two or more half-lives. The turnover frequency N_t (h^{-1}) was calculated from the slope m of the least-squares determined line [N_t = (60 min h^{-1})/m], fit to one half-life because of product inhibition observed (in some cases) at higher conversions. Reported turnover frequencies are the average of at least two kinetic runs.

Table 1. Summary of the Crystal Structure Data for [Cp′$_2$YP(H)Ph]$_2$ (**20**)

formula	$C_{52}H_{72}P_2Y_2$
cryst syst	tetragonal
space group	$P4_2/m$
a, b	11.1734(12) Å
c	19.129(3) Å
V	2388.3(4) Å^3
Z	4
d_{calc}	1.27 g/cm^3
crystal size, mm	0.15 × 0.13 × 0.10
color, habit	colorless, trigonal bipyramidal
diffractometer	Bruker SMART-1000 CCD
temp	−120 °C
μ	25.2 cm^{-1}
transmission factors, range	0.7376−0.8132
radiation	Mo Kα (λ = 0.71069 Å)
exposure time	25 s
scan width	0.30°
2θ range	56.5°
intensities (unique, R_i)	22200 (3033, 0.163)
intensities > 3σ	1203
no. of params	124
R	0.067
R_w^2 [$\Sigma(w(F_0^2 - F_C^2)^2)/[\Sigma(w(F_0^2)^2]^{1/2}$	0.138
min, max density in ΔF map	−0.65, 1.07 e$^-$/Å^3

Results

The goal of this study was to examine in detail the viability, selectivity, rates, and mechanism of hydrophosphination/cyclization processes mediated by organolanthanide catalysts. This section first presents general synthetic routes to the organophosphine substrates and the activation of the organolanthanide precatalysts. Next, the catalytic intramolecular hydrophosphination/cyclization of these phosphines is described, including the scope of the transformation, as well as the effects of varying the metal center and ancillary ligands. Reaction kinetics and mechanistic pathways are then discussed, followed by regio- and diastereoselectivity, and finally the resting state and molecular structure of the catalyst. The Discussion section brings together various aspects of the catalytic cycle, and compares and contrasts the results of this study with well-developed, organolanthanide-mediated hydroamination systems.[11−13]

Substrate Synthesis. To investigate hydrophosphination/cyclization processes with organolanthanide catalysts in detail, suitable phosphinoalkene and phosphinoalkyne substrates were required. Primary and secondary phosphines are air-sensitive and difficult to handle, and the reported synthetic routes are not general.[38] Therefore, a general method for the synthesis of primary phosphines was developed, consisting of two basic steps. First an air-stable phosphonate was synthesized by either

(34) Lowen, G. T.; Almond, M. R. *J. Org. Chem.* **1994**, *59*, 4548−4550.
(35) Patois, C.; Savignac, P. *Bull. Soc. Chim. Fr.* **1993**, *130*, 630−635.
(36) Cromer, D. T.; Waber, J. T. *International Table for X-ray Crystallography*; The Kynoch Press: Birmingham, England, 1974; Vol. IV.
(37) *SIR92*: Altomare, A.; Cascarano, M.; Giacovazzo, C.; Guagliardi, A. *J. Appl. Crystallogr.* **1993**, *26*, 343−350.
(38) Syntheses of primary and secondary phosphines: (a) Reference 23. (b) Cabioch, J. L.; Denis, J. M. *J. Organomet. Chem.* **1989**, *377*, 227−233. (c) Wolfsberger, W. *Chem.-Ztg.* **1988**, *12*, 379−381. (d) Kosolapoff, G. M.; Maier, L. *Organic Phosphorus Compounds*; Wiley-Interscience: New York, 1972; Vol. 1, pp 1−287.

Scheme 3. Synthesis of Phosphine Substrates; Illustrated for Substrates **1**, **3**, and **13**

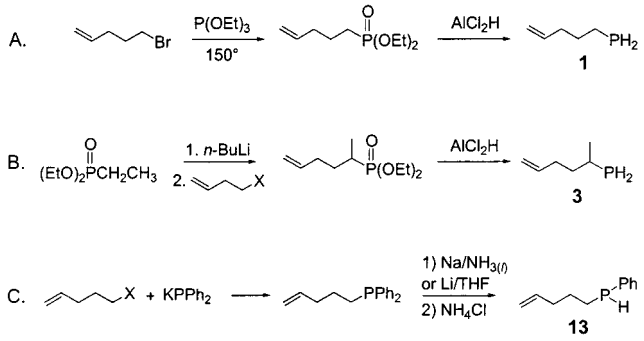

of two methods (Scheme 3). Method A employs the Arbuzov reaction of a phosphite with an alkyl halide,[39] and the only complication is synthesis of the corresponding alkenyl or alkynyl fragment. Method B involves α-deprotonation of an alkyl phosphonate, followed by electrophilic addition of the appropriate alkyl chain and is more effective for formation of substrates having branched hydrocarbon backbones.[35] In either case, the resulting phosphonate is then reduced with "dichloroalane" $AlCl_2H$ (in this case a 5:2 molar mixture of $AlCl_3$ and $LiAlH_4$),[40] followed by anaerobic workup with deoxygenated water. Substrates containing a phenyl group can be isolated by removal of the diethyl ether solvent; however, more volatile phosphines cannot be easily separated from common organic solvents and instead were isolated by vacuum-transfer away from a high-boiling tetraglyme-based reducing mixture. Secondary phenylphosphines were also synthesized (Method C) by first reacting $KPPh_2$ with the appropriate alkyl halide and then cleaving a phenyl group from the resulting tertiary phosphine using an alkali metal reagent.[41] All phosphine substrates were stored as solutions in C_6D_6 or C_7D_8, and the solutions were dried over several portions of freshly activated molecular sieves. They were characterized by ^1H, ^{13}C, and ^{31}P NMR, high-resolution mass spectrometry, and elemental analysis (when possible) as detailed in the Experimental Section.

Catalyst Generation. $Cp'_2LnE(TMS)_2$ precatalysts (E = N, CH) have been used extensively for intra-and intermolecular hydroamination, and entry to the catalytic cycle is known to proceed via rapid and quantitative protonolysis of the Ln−E σ bond, with concomitant formation of a new Ln−N σ bond (step *i*, Scheme 1).[11−13] Although all evidence supports a proposed catalytic cycle for hydrophosphination which is similar (Scheme 2), we observe that initial protonolysis of the Ln−E bond by primary and secondary phosphine substrates is *far slower than by amine substrates* (step *i*, Scheme 2). Thus, while mM Ln−$CH(TMS)_2$ protonolysis by mM primary and secondary amines is essentially instantaneous at −78 °C, we find that half-lives for the corresponding mM Ln−$CH(TMS)_2$ protonolysis by mM phosphine reagents can be minutes to hours at room temperature, depending on substrate structure and also depending on substrate and catalyst concentrations (Figure 1). This rate-ordering appears to be a consequence of the weaker product Ln−P bond compared to the Ln−N bond,[19] as well as the softer nature of phosphorus compared to nitrogen, suggesting a weaker interaction with the hard Ln^{3+} metal center.[42] Primary phosphines are reported to be slightly stronger Brønsted acids than primary amines;[43] however, it appears that hard−soft effects and also perhaps the somewhat greater steric bulk of the organophos-

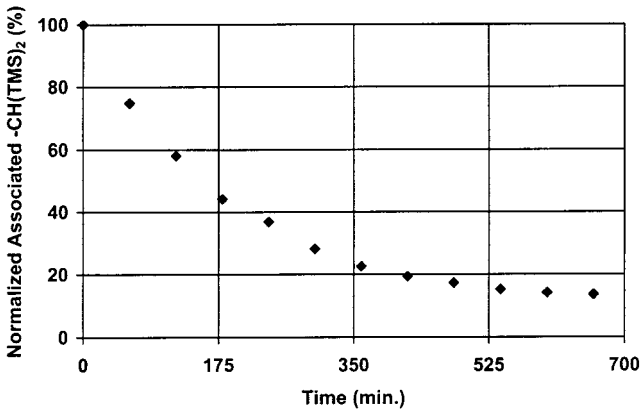

Figure 1. Plot of the reaction of precatalyst $Cp'_2YCH(TMS)_2$ with ~30 equiv of *n*-pentyl phosphine (**19**) at 25 °C in C_7D_8.

Table 2. Scope of Organolanthanide-Catalyzed Hydrophosphination/Cyclization of Phosphinoalkenes and Phosphinoalkynes[a]

entry	substrate	product	N_t, h^{-1} (°C)
1.	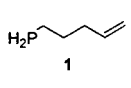 1	 2	2.2 (22)[c] 50.1 (25)[d]
2.	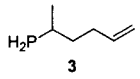 3	 4	49.9 (25)[c] ~ 340 (25)[d]
3.	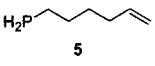 5	 6	11.8 (25)[c] 91.3 (25)[d]
4.	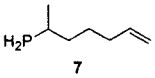 7	 8	6.6 (22)[c] 16.0 (25)[d]
5.	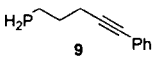 9	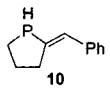 10	12.4 (22)[b] 2.03 (40)[c] 0.08 (40)[d] 13.5 (22)[e]
6.	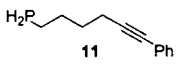 11	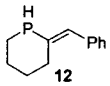 12	4.4 (22)[b]
7.	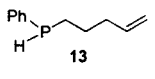 13	 14	0.25 (40)[b]
8.	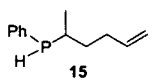 15	 16	~0.05 (60)[b]
9.	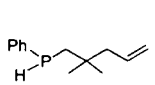 17	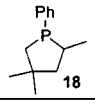 18	0.18 (40)[b]

[a] All turnover frequencies (N_t) measured in C_6D_6. Conversion is >95% by ^1H and ^{31}P NMR spectroscopy. [b] $Cp'_2LaCH(TMS)_2$ as precatalyst. [c] $Cp'_2SmCH(TMS)_2$ as precatalyst. [d] $Cp'_2YCH(TMS)_2$ as precatalyst. [e] $Me_2Si(Me_4C_5)(^tBuN)SmN(TMS)_2$ as precatalyst.

(39) (a) Delamarche, I.; Mosset, P. *J. Org. Chem.* **1994**, *59*, 5453−5457. (b) Bhattacharya, A. K.; Thyagarajan, G. *Chem. Rev.* **1981**, *81*, 415−430.
(40) Ashby, E. C.; Prather, J. *J. Am. Chem. Soc.* **1966**, *88*, 729−733.
(41) (a) Na/NH_3: ref 38c. (b) Li/THF: Chou, T.-S.; Yuan, J.-J.; Tsao, C.-H. *J. Chem. Research (S)* **1985**, 18−19. (c) Li and Na cleavage methods: Budzelaar, P. H. M.; Doorn, J. A.; Meijboom, N. *Recl. Trav. Chim. Pays-Bas* **1991**, *110*, 420−432.
(42) (a) Pearson, R. G. *J. Chem. Educ.* **1987**, *64*, 561−567. (b) Ho, T.-L. *Hard and Soft Acids and Base Principles in Organic Chemistry*, Academic Press: New York, 1977. (c) Pearson, R. G. *Hard and Soft Acids and Bases*, Dowden, Hutchinson, and Ross, Inc: Straudsburg, 1973.

phorus reagents compared to those of nitrogen are the dominant factors. The lanthanide ionic radius is also important in this initiation step, and $-E(TMS)_2$ cleavage is more rapid for the larger metal ions (La^{3+}, Nd^{3+}) and increasingly sluggish as the ionic radius is decreased (Y^{3+}, Lu^{3+}).

The most effective way to activate bis-Cp′ hydrocarbyl complexes completely and immediately for catalytic studies is to generate the corresponding hydride $(Cp'_2LnH)_2$ in situ using H_2[5a] and to then expose this catalyst to the phosphine substrate. Using this protocol, immediate Ln−P bond formation occurs, and the $H_2C(TMS)_2$ generated via hydrogenolysis can be used as an internal NMR standard to monitor the course of the reaction (via the substrate:catalyst ratio). Color changes are also observed which indicate Ln−P bond formation; for example, a yellow $(Cp'_2LaH)_2$ solution becomes orange when it undergoes reaction with a phosphine substrate, while red $(Cp'_2YH)_2$ solutions turn bright yellow. Unlike the amine hydroamination/cyclizations,[11−13] the hydrophosphination reaction mixtures do not return to the initial colors when substrate consumption is complete, except at very low (≤10:1) ratios of substrate:catalyst. All of the present phosphine-based cyclizations proceed until complete conversion (>95%) of the substrate has occurred (assayed by ^1H and ^{31}P NMR). No catalyst decomposition is observed, and as long as the reaction medium is free of air and moisture, turnover continues.

Scope of Catalytic Hydrophosphination/Cyclization. Alkenyl phosphine substrates undergo efficient cyclization in the presence of organolanthanide catalysts to afford phospholane and phosphorinane products (Table 2). Phospholanes (fully saturated five-membered phosphorus-containing rings; entries 1, 2, 7, 8, 9) and phosphorinanes (fully saturated six-membered phosphorus-containing rings, entries 3, 4) are formed cleanly and efficiently from alkenyl phosphines. Turnover frequencies are roughly similar to those observed for analogous aminoalkenes, although the dependence on ring size is not strictly 5 > 6, as observed for hydroamination/cyclization reactions.[11−13] The reactions proceed until starting material is completely consumed; however, formation of a noncatalytic side product is also observed (eq 1). Varying quantities of a larger endocyclic

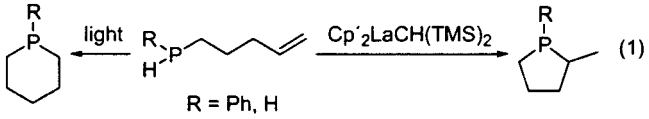

(1)

ring are formed during substrate drying and storage; however, this does not interfere with the catalytic reaction. This side product could be formed independently by heating the substrate and exposing it to light, and multinuclear NMR with reference to literature data[44] was used to confirm the phosphorinane assignment. There is precedent for such endocyclization processes which are thought to be radical chain in nature;[45] however, storing the present phosphinoalkenes with small quantities of the radical inhibitor hydroquinone does not significantly inhibit this process. Light and heat both accelerate this side reaction, and therefore, the present phosphine substrates were protected from light both before and during catalytic reactions. Substrates **1**, **3**, **13**, **15**, and **17** are affected in varying degrees by this competing, apparently noncatalytic process, and in some cases **1** and **3** afford these byproducts in significant quantities, as will be discussed below. Alkynyl substrates are not susceptible to this reaction, and olefinic substrates **5** and **7**, which would form less kinetically/thermodynamically favorable seven-membered rings, do not undergo this side reaction at a measurable rate, even upon heating. Attempts were also made to effect catalytic cyclizations of hept-6-enylphosphine (**C**) and 1-methyl-hept-6-enylphosphine (**D**) to the corresponding seven-membered rings; however, the reactions are sluggish and, upon extended heating to 60 °C, these substrates undergo noncatalytic oligomerization and decomposition reactions. Therefore, the scope of intramolecular hydrophosphination/cyclization is currently limited to the formation of five- and six-membered phosphorus-containing heterocycles.

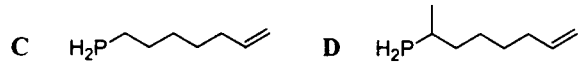

Alkynyl phosphines also undergo clean and efficient cyclizations (Table 2, entries 5, 6). In this case, five-membered ring **10** is formed more rapidly than is six-membered ring **12**, in accord with the trend observed for aminoalkynes.[12] However, products **10** and **12** are unstable and within hours undergo dimerization. This dimerization process is not catalyst- or light-dependent, and several ultimate products are detected by GC−MS, all having parent ion molecular masses indicative of dimers. Although the mechanism of the dimerization has not been rigorously defined, a possible route could begin with isomerization of the product to a phospha-alkene (not observed; analogous to the enamine−imine tautomerization previously observed in the cyclization of aminoalkynes[12b,46]), and phospha-alkenes are known to add to P═C and C═C bonds (eq 2).[47]

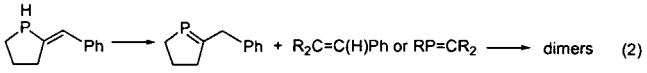

(2)

Terminal alkynyl substrate 4-pentynylphosphine (**E**) was also investigated. This substrate undergoes concurrent cyclization and oligomerization (eq 3), with the latter process presumably analogous to that previously observed for organolanthanide-mediated oligomerization of simple terminal alkynes.[47] Therefore, an accurate quantitation of the turnover frequency for the hydrophosphination/cyclization process could not be obtained, although qualitatively it is a very rapid process (N_t > 100/h^{-1}). The cyclized product also undergoes rapid dimerization (determined by GC−MS), as observed for phosphinoalkyne cyclization products **10** and **12**.

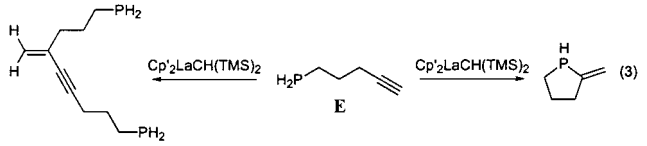

(3)

Metal and Ancillary Ligand Effects on Catalytic Hydrophosphination/Cyclization. Depending upon the substrate type, organolanthanide-mediated hydroamination/cyclization processes exhibit distinctive trends in turnover frequency with metal ionic radius; increasing ionic radii correlates with greater

(43) The Brønsted acidities of some primary and secondary phosphines and amines have been compared, and phosphines are generally slightly more acidic: Issleib, K.; Kümmel, R. *J. Organomet. Chem.* **1965**, *3*, 84−91.

(44) The chemical shifts of phospholanes and phosphorinanes are known to be different; see ref 15. In addition, the side product formed by the endocyclic reaction of **3** is identical to the catalytic product formed in organolanthanide-catalyzed cyclization **5** → **6**.

(45) Examples of P−H addition to olefins to form phospolanes and phosphorinanes: (a) Hackney, M. L.; Schubert, D. M.; Brandt, P. F.; Haltiwanger, R. C.; Norman, A. D. *Inorg. Chem.* **1997**, *36*, 1867−1872. (b) Brandt, P. F.; Schubert, D. M.; Norman, A. D. *Inorg. Chem.* **1997**, *36*, 1728−1731. (c) Field, L. D.; Thomas, I. P. *Inorg. Chem.* **1996**, *35*, 2546−2548. (d) Davies, J. H.; Downer, J. D.; Kirby, P. *J. Chem. Soc. (C)* **1966**, 245−247.

Table 3. Metal Ion Size Effects on Turnover Frequencies for the Hydrophosphination/Cyclization of Substrates **1** and **9**

catalyst	ionic radius[a]	N_t, h^{-1} (°C)[b] 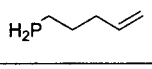	N_t, h^{-1} (°C)[b] 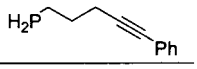
Cp'_2La-	1.160 Å	0.90 (40)	12.4 (22)
Cp'_2Sm-	1.079 Å	2.2 (22)	2.03 (40)
Cp'_2Y-	1.019 Å	50.1 (25)	0.08 (40)
Cp'_2Lu-	0.977 Å	4.4 (25)	

[a] Eight-coordinate ionic radii from reference 2. [b] All rates measured in C_6D_6.

turnover frequencies for aminoalkenes,[11] whereas decreasing ionic radii correlate with greater turnover frequencies for aminoalkynes,[12] and lanthanides with intermediate ionic radii exhibit the highest turnover frequencies for aminoallenes.[13] The phosphinoalkynes studied here exhibit behavior similar to that of aminoalkenes, with larger metal ions affording greater turnover frequencies (Table 3). Phosphinoalkenes, however, exhibit a different trend in that the mid-sized Y^{3+} ion exhibits the highest N_t values, followed by Lu^{3+} and Sm^{3+}, with the largest La^{3+} ion the most sluggish (Table 3). The effects of ancillary ligands on reaction rates also differ markedly between phosphinoalkynes and phosphinoalkenes, in that opening the catalyst coordination sphere with the $Me_2Si(Me_4C_5)(^tBuN)Ln-$(CGC; **F**) ligand leads to enhanced cyclization rates for alkynes (Table 2, entry 5). In contrast, for phosphinoalkenes little catalytic activity is observed with CGC complexes, and turnover

F 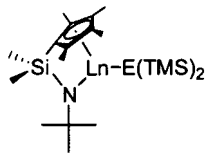

rates are too sluggish to measure. Qualitatively, the same is true using the sterically open $Me_2SiCp''_2NdCH(TMS)_2$ catalyst, in that it leads to enhanced rates for phosphinoalkyne cyclization, but depressed rates are observed with phosphinoalkenes. Thus, it appears that phosphinoalkynes are activated and undergo cyclization via a pathway similar to that for aminoalkenes,[11] while phosphinoalkene cyclizations are more sensitive to catalyst structural variations, and large changes in turnover frequencies occur with small changes in metal ion size and ancillary ligation.

Kinetic and Mechanistic Studies of Hydrophosphination/Cyclization. Quantitative kinetic studies of the cyclizations of the various phosphine substrates were carried out and monitored by ^1H and ^{31}P NMR spectroscopy. Both Y^{3+} and Sm^{3+} catalysts were used, with each offering distinctive advantages. In the case of diamagnetic $Cp'_2YCH(TMS)_2$, integration of the resonances is straightforward, while for paramagnetic $Cp'_2SmCH(TMS)_2$, broadening of some resonances provides information about which portions of the substrate and product structures interact closely with the metal center. The cyclization reactions were carried out with a 30−150-fold molar excess of substrate, and in all cases substrate was completely consumed. The decrease of olefinic (δ ~5.8 ppm) or P−H (δ ~3.5 ppm) resonances

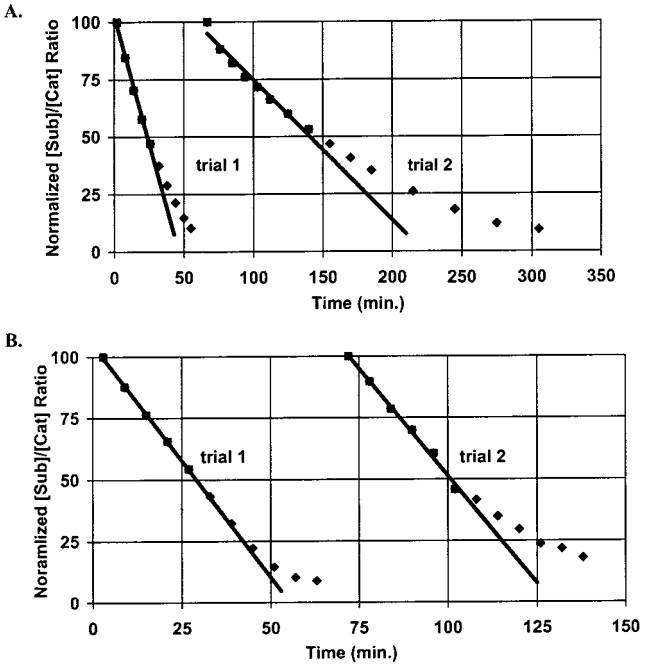

Figure 2. Kinetics of organolanthanide-mediated hydrophosphination/cyclization. (A) Cyclization of pent-4-enylphosphine (**1** → **2**) mediated by H_2-activated $Cp'_2YCH(TMS)_2$ in C_6D_6 at 25 °C. The lines represent the least-squares fit to the data points for the first half-life of the reaction. (B) Cyclization of 1-methylpent-4-enylphosphine (**3** → **4**) mediated by H_2-activated $Cp'_2SmCH(TMS)_2$ in C_6D_6 at 25 °C. The lines represent the least-squares fit to the data points for the first half-life of the reaction. The deviation from zero-order kinetics is ascribed to competitive inhibition by product (see text).

was monitored over time and normalized versus the $CH_2(TMS)_2$ internal standard (δ ~0.05 ppm) produced by catalyst activation. The data show that the rate of substrate consumption is initially zero-order in substrate concentration; however, after approximately one half-life, deviations suggestive of competitive inhibition by product[11] are observed. These kinetic inhibition effects are less evident at higher temperatures, more marked at lower temperatures, and also depend on the steric bulk of the product. As an example, the **1** → **2** cyclization with H_2-activated precatalyst $Cp'_2YCH(TMS)_2$ was monitored until complete consumption of **1**, then an additional aliquot of **1** was added to the same reaction mixture, and monitoring of the reaction continued (Figure 2A). Likewise, the cyclization of **3** → **4** with H_2-activated precatalyst $Cp'_2SmCH(TMS)_2$ was carried out in the same way (Figure 2B). These measurements show inhibition (deviation from zero-order kinetics) in the **1** → **2** cyclization (Figure 2A) after one half-life in the first data set and more severe inhibition in the second data set, where substantial concentrations of product **2** are now present. In contrast, Figure 2B evidences substantially less inhibition for the **3** → **4** cyclization in either the first or second data set, suggesting that the increased steric bulk of phospholane **4** (relative to **2**) renders it a less effective inhibitor. There is no decrease in initial catalytic activity in the second data set for the **3** → **4** cyclization; therefore, no catalyst decomposition is evident. ^1H and ^{31}P NMR spectra also reveal that both substrate and product resonances are broadened in cyclizations mediated by paramagnetic catalysts, in contrast to the analogous hydroamination results where only substrate resonances are severely broadened.[11−13] Because no detectable catalyst decomposition occurs in these reactions, the observed deviation from linearity in the reaction kinetics is most reasonably assigned to product inhibition. However, for all cyclizations studied, data for at least the first half-life indicate

(46) Tautomerization of enamines to imines: (a) Lammertsma, K.; Prasad, B. V. *J. Am. Chem. Soc.* **1994**, *116*, 642−650. (b) Shainyan, B. A.; Mirskova, A. N. *Russ. Chem. Rev.* **1979**, *48*, 107−117.

(47) a) Mackewitz, T. W.; Regitz, M. *Synthesis* **1998**, 125−133. (b) Mackewitz, T. W.; Peters, C.; Bergsträsser, U.; Leininger, S.; Regitz, M. *J. Org. Chem.* **1997**, *62*, 7605−7613. (c) Mackewitz, T. W.; Regitz, M. *Liebigs Ann.* **1996**, 327−333. (d) Slany, M.; Regitz, M. *Synthesis* **1994**, 1262−1266.

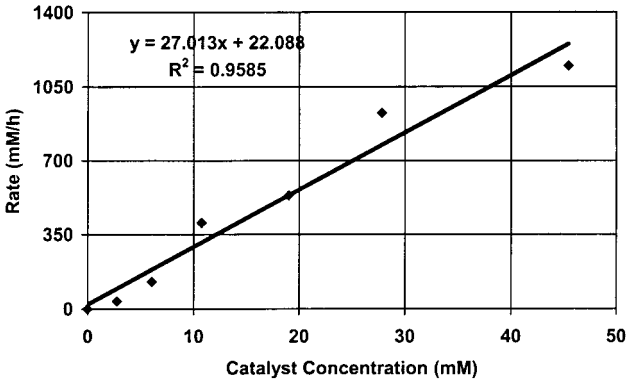

Figure 3. Determination of reaction order in lanthanide concentration for the hydrophosphination/cyclization of pent-4-enylphosphine (**1** → **2**) mediated by H_2-activated $Cp'_2YCH(TMS)_2$ in C_6D_6. The line represents the least-squares fit to the data points.

the reaction to be approximately zero-order in substrate concentration. Attempts to fit the kinetic data to other simple rate laws (e.g., first-order in substrate concentration) yielded results which were less convincing.

A plot of reaction rate versus precatalyst concentration for the **1** → **2** cyclization mediated by H_2-activated $Cp'_2YCH(TMS)_2$, in which substrate concentration is held constant and precatalyst concentration varied over a more than 10-fold range, shows the reaction to be first-order in catalyst concentration (Figure 3). Overall, the empirical rate law (eq 4) is essentially the same

$$\nu = k[\text{substrate}]^0[\text{catalyst}]^1 \qquad (4)$$

as was observed for hydroamination,[11−13] although competing kinetic inhibition by the phosphorus heterocyclic product is more pronounced. Variable-temperature kinetic measurements were also carried out for the **3** → **4** cyclization mediated by H_2-activated $Cp'_2SmCH(TMS)_2$ and indicate the reaction to be approximately zero-order in substrate concentration over a greater than 30 °C temperature range (Figure 4A). Arrhenius and Eyring (Figure 4B) analyses afford the activation parameters $E_a = 13.0$ (1.4) kcal/mol, $\Delta H^{\ddagger} = 12.3$ (1.6) kcal/mol, and $\Delta S^{\ddagger} = -25.9$ (5.2) eu.

Reaction Selectivity. The catalytic cyclization of a phosphinoalkene generates a new stereocenter at carbon, with an additional stereocenter generated because of the slow inversion at phosphorus,[49] meaning that, in principle, two diastereomers (two pairs of enantiomers) can be formed in the **1** → **2** cyclization (eq 5). The selectivity for phosphinoalkene ring

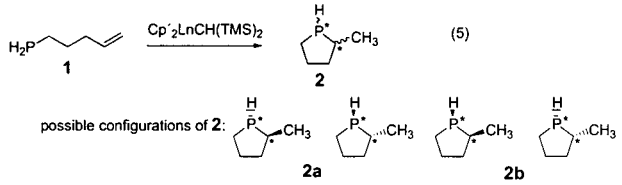

closure is highly catalyst-dependent only for substrate **3** while for substrates **1**, **5**, and **7** the ratios of product diastereomers are essentially invariant with catalyst (Table 4). All ratios are invariant with conversion as assayed by ^{31}P NMR and also do

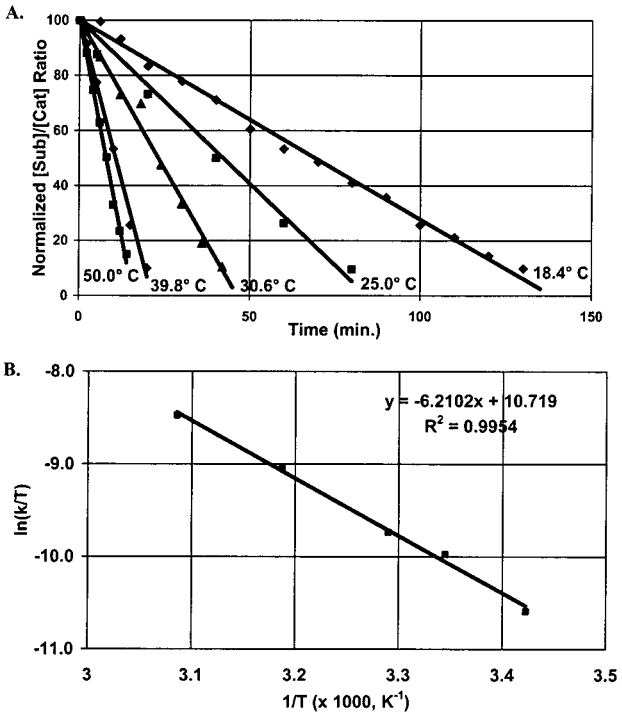

Figure 4. (A) Normalized ratio of substrate to lanthanide concentration as a function of time and temperature for the hydrophosphination/cyclization of 1-methyl-pent-4-enylphosphine (**3** → **4**) using H_2-activated precatalyst $Cp'_2SmCH(TMS)_2$ in C_6D_6. (B) Eyring plot for the hydrophosphination/cyclization of 1-methyl-pent-4-enylphosphine (**3** → **4**) using H_2-activated precatalyst $Cp'_2SmCH(TMS)_2$ in C_6D_6. The lines are least-squares fits to the data points.

Table 4. Effect of Catalyst on *cis/trans* Selectivity of Hydrophosphination at 25 °C

entry	substrate	possible exocyclic products	catalyst	distribution (%) a	b	c
1.	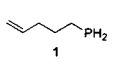	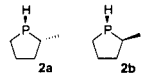	Cp'_2La-	28	52	-
			Cp'_2Sm-	34	60	-
			Cp'_2Y-	29	54	-
			Cp'_2Lu-	20	33	-
2.	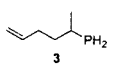	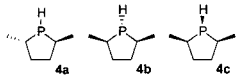	Cp'_2La-	12	30	trace
			Cp'_2Sm-	72	17	trace
			Cp'_2Y-	35	53	trace
			Cp'_2Lu-	26	64	trace
			Cp'_2Sm-[a]	44	46	3
			Cp'_2Y-[a]	64	12	19
			Cp'_2Lu-[a]	76	8	8
3.	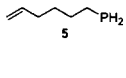	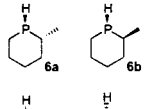	Cp'_2Sm-	89	11	-
			Cp'_2Y-	89	9	-
4.	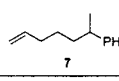	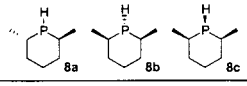	Cp'_2Sm-	12	86	2
			Cp'_2Y-	11	77	12

[a] Added ∼10 equiv *n*-propylamine.

not change after completion of the reaction (in the presence of catalyst or after separation from the catalyst). The ^{31}P chemical shifts of the various products are substantially dispersed, allowing accurate NMR assay of the product distributions.[50] Phospholane **2** is consistently produced in an approximate 2:1 ratio of **2b** : **2a** (Table 4, entry 1), regardless of the catalyst. The product phospholane configuration is assigned by 2D-NOESY spectroscopy and coupling constant analysis.[29,51] In addition, the *cis/trans* configurational disposition of **2** is implied

(48) Heeres, H. J.; Teuben, J. H. *Organometallics* **1991**, *10*, 1980−1986.

(49) The barrier to inversion at phosphorus is typically about 35 kcal/mol: (a) Reference 15a. (b) Baechler, R. D.; Mislow, K. *J. Am. Chem. Soc.* **1970**, *92*, 3090−3093. (c) Rauk, A.; Allen, L. C.; Mislow, K. *Angew. Chem., Int. Ed. Engl.* **1970**, *9*, 400−414.

(50) The present phospholanes with different configurations have chemical shift differences of 10−15 ppm, and phosphorinanes are generally downfield of phospholanes in ^{31}P NMR: see ref 15.

(51) For details on the assignment of the configuration of **2**, please see the Experimental Section.

by ^{31}P NMR spectroscopy in the presence of a paramagnetic catalyst, since the phosphorus lone pair should be more accessible for the *cis* configuration than the *trans* and therefore should interact more strongly with the catalyst. Indeed the *cis*-**2b** resonance is appreciably broader.

The distribution of phospholane product **4** stereoisomers (Table 4, entry 2) exhibits a large variation with metal ion size—as high as 70% **4a** for Cp'_2Sm-, a marginal selectivity for Cp'_2Y-, and greater than 60% **4b** for Cp'_2Lu-.[30] A trace quantity of a third phospholane, presumably **4c**, is observed in all cases. Decreasing the reaction temperature to 0 °C does not effect a significant change in product ratios for the **1** → **2** and **3** → **4** cyclizations mediated by Cp'_2Y- and Cp'_2Sm-. Addition of ~10 equiv of *n*-propylamine to the **3** → **4** cyclization also results in a large change in selectivity, with a nearly 1:1 mix of **4a** and **4b** with Cp'_2Sm-, and high selectivities for **4a** with both Cp'_2Y- and Cp'_2Lu-.[52] Six-membered phosphorinanes **6** and **8** are both obtained in greater than 80% diastereoselectivity (**6a** and **8b**, entries 3, 4, Table 4) regardless of catalyst. Secondary phenylphosphines **14**, **16,** and **18** undergo sluggish cyclization and yield catalyst-invariant diastereomeric ratios of ~10:1, 1:1, and 1:1, respectively.

As noted above (eq 1), noncatalytic endocyclic ring formation is also observed for substrates **1** and **3**, and accounts for the remainder of the product mixture (not tabulated) in Table 4. In most cases, this product represents 10−15% of the total and is largely formed during the drying of the substrate, and not during the catalytic reaction. However, in a few lanthanocene cases (**1** → **2** mediated by Cp'_2Lu-; **3** → **4** mediated by Cp'_2La-) and also when more open ancillary ligand systems such as the CGC ligand[3a] and the chiral $Me_2Si(Cp'')(CpR^*)$ ligand[4] are employed, minor formation of the exocyclic product and predominant formation of the endocyclic product are observed. Possible reasons and a possible alternate mechanistic pathway are considered in the Discussion section.

Catalyst Resting State. Initial observations regarding the catalyst resting state were made using paramagnetic metal centers Nd^{3+} and Sm^{3+}. The substrate P−H resonances are broadened throughout the course of the reaction, indicating rapid exchange of bound and free P−H species. At an initial level of analysis, a phosphine−phosphido resting state for the catalyst (**G**), analogous to the amine−amido resting state established for hydroamination (**H**),[11] seems most reasonable. Broadening of the heterocyclic product P−H signals indicates that these phosphines undergo rapid coordination to/dissociation from, the lanthanide metal center, also paralleling the amine−amido system.

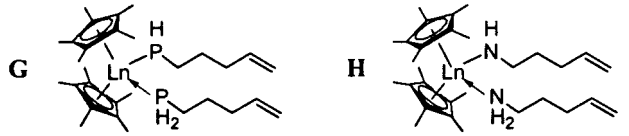

To examine the resting state of the present hydrophosphination catalysts in greater detail, low-temperature ^{1}H and ^{31}P NMR studies were undertaken. The diamagnetic catalyst $(Cp'_2YH)_2$ was chosen because ^{89}Y has $I = {}^1/_2$ (100% natural abundance) and because several examples of Y−P bonds are known.[53] Only a few transition metal phosphine−phosphido complexes have been reported, chemical shifts are not diagnostic, and phosphido ($M-PR_2$) ligand ^{31}P chemical shifts can range over more than 100 ppm,[53,54] while phosphine ($M-PR_3$) ligands exhibit ^{31}P NMR resonance positions similar to those of the analogous free phosphine. However, the multiplicities observed in the NMR give useful information about the nature of species in solution, and diagnostic coupling constants are in the range $^1J_{^{31}P-^{89}Y} \approx 50-70$ Hz (e.g., **J**[53a]), $^1J_{^{31}P-^1H} \approx 180-200$ Hz,[15] and $^2J_{^1H-^{89}Y} \approx 2-3$ Hz.[55]

Table 5. Chemical Shifts[a] and Coupling Constants for the Reactions of Phosphines with $(Cp'_2YH)_2$ at −80 °C

species	δ, ppm	J, ^{31}P{^{1}H}, Hz	J, ^{31}P−^{1}H, Hz
K	−17.4	d, 126	d, 214
L	−90.1	d of d, 87, 58	d, 189
M	−110.2	multiplet	multiplet
N	−37.5	d of d, 384, 51	d, 302
	−81.6	d of d, 384, 45	none
O	−33.7	d, 110	d, 206
	−39.4	d, 68	d, 272
P	−20.3	d, 70	d, 267
	−24.1	d, 124	d, 205

[a] Chemical shifts reported relative to an external 85% H_3PO_4 standard.

J

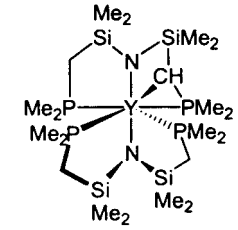

Phosphinoalkene **1** was investigated initially; however, the data proved difficult to interpret since the presence of the endocyclic ring side product, as well as the onset of catalytic cyclization at higher temperatures (≥−20 °C), severely complicate the spectra. Therefore, the noncyclizable phosphines $PhPH_2$ and $H_2PCH_2(CH_2)_3CH_3$ (**19**) were investigated, as models for the actual substrates. $(Cp'_2YH)_2$ was generated in situ and treated with the phosphine in a ~10:1 molar ratio at −78 °C. Spectra were recorded initially at −80 °C and then at higher temperatures as the mixture was gradually warmed to 25 °C. ^{1}H NMR spectra were complex and not particularly informative over the temperature range, while ^{31}P data were more informative and are tabulated with coupling constants in Table 5.

The low-temperature ^{31}P{^{1}H} spectrum of the $(Cp'_2YH)_2$ + **19** reaction mixture (Figure 5A) reveals a doublet ($J = 126$ Hz) at δ −17.4 ppm (**K**), while the ^{1}H-coupled spectrum (Figure 5B) reveals **K** as a doublet of doublets ($J_1 = 214$ Hz, $J_2 = 126$ Hz). These data indicate a Y−P bond, with the proton-coupled spectrum indicating that a single P−H linkage is also present. By analogy to the lanthanocene alkylamido hydroamination chemistry[11] and as evidenced by phosphine broadening in the presence of paramagnetic lanthanocene catalysts, there are likely additional phosphorus ligands (presumably phosphines) coordinated to the metal center; however, they must be exchanging

(52) Not surprisingly, addition of *n*-propylamine slows the rate of reaction; see ref 11a.

(53) For examples, see: (a) Fryzuk, M. D.; Haddad, T. S.; Rettig, S. J. *Organometallics* **1991**, *10*, 2026−2036. (b) Fryzuk, M. D.; Haddad, T. S. *J. Am. Chem. Soc.* **1988**, *110*, 8263−8265. (c) Westerhausen, M.; Hartmann, M.; Schwarz, W. *Inorg. Chim. Acta* **1998**, *269*, 91−100.

(54) (a) Cole, M. L.; Hibbs, D. E.; Jones, C.; Smithies, N. A. *J. Chem. Soc., Dalton* **2000**, 545−550. (b) Zwick, B. D.; Dewey, M. A.; Knight, D. A.; Buhro, W. B.; Arif, A. M.; Gladysz, J. A. *Organometallics* **1992**, *11*, 2673−2685.

(55) $^2J_{^{89}Y-^1H}$ couplings are typically very small and are frequently not observed. See: a) Bambirra, S.; Brandsma, M. J. R.; Brussee, E. A. C.; Meetsma, A.; Hessen, B.; Teuben, J. H. *Organometallics* **2000**, *19*, 3197−3204. (b) den Haan, K. H.; Boer, J. L.; Teuben, J. H.; Spek, A. L.; Jojiæ-Prodiæ, B.; Hays, G. R.; Huis, R. *Organometallics* **1986**, *5*, 1726−1733.

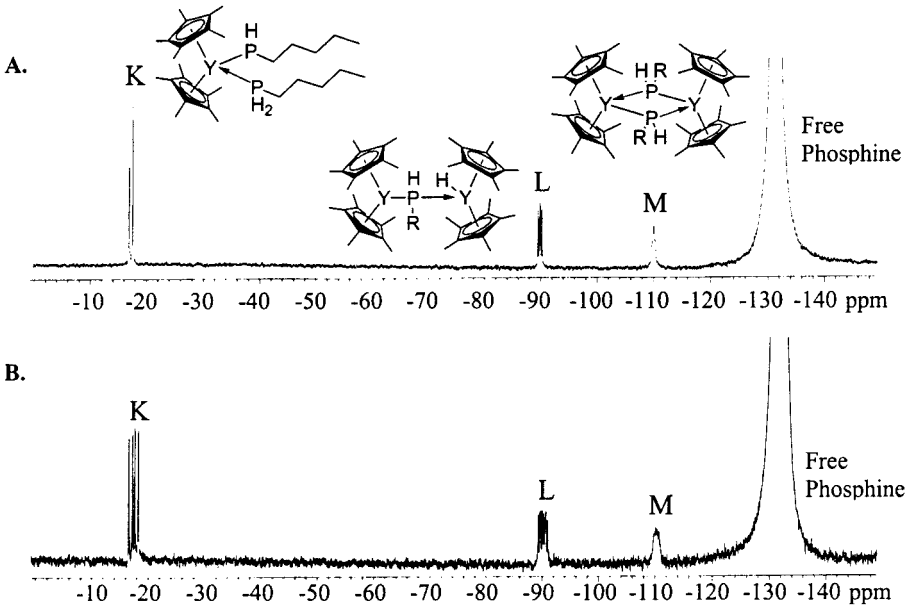

Figure 5. (A) Low-temperature (−80 °C) $^{31}P\{^1H\}$ spectrum of an *n*-pentylphosphine + $(Cp'_2YH)_2$ reaction mixture in C_7D_8. (B) Low-temperature (−80 °C) $^{31}P-^1H$-coupled spectrum of an *n*-pentylphosphine + $(Cp'_2YH)_2$ reaction mixture in C_7D_8. R = *n*-pentyl in the Figure.

with free phosphine at a rate which is rapid on the ^{31}P NMR time scale, even at −80 °C. These results suggest a phosphine−phosphido catalyst resting state such as **K**, analogous to that identified in organolanthanide-mediated hydroamination,[10a] **H**.

K

The next higher field $^{31}P\{^1H\}$ resonance (Figure 5A) is a doublet of doublets (J_1 = 87 Hz, J_2 = 58 Hz) at δ −90.1 ppm (**L**), which expands to a doublet of doublet of doublets (J_1 = 189 Hz, J_2 = 87 Hz, J_3 = 58 Hz) in the ^1H-coupled spectrum (Figure 5B). This resonance decreases in relative intensity as the solution is warmed and is not detectable by ca. −10 °C. Importantly, this peak is *not* observed upon recooling the solution to −80 °C, whereas signals **K** and **M** reversibly increase and decrease (with broadening) in intensity with cooling and warming, respectively. The solution gradually changes color upon warming, from the red color of $(Cp'_2YH)_2$ solutions to an orange color and gradually to the final yellow color indicative of Y−P bond formation. Furthermore, the yellow color does not revert to red upon recooling. These results suggest that this resonance arises from initial Y−P bond formation, a sluggish process at low temperatures. The ^{31}P doublet of doublets is consistent with two inequivalent Y^{3+} metal centers, and the increased multiplicity in the ^1H-coupled spectrum indicates a P−H linkage is also present, suggesting a structure such as **L**.

L R = *n*-pentyl

The final $^{31}P\{H\}$ resonance observed, aside from free *n*-pentyl phosphine at δ −132 ppm, is a multiplet at δ −110.2 ppm (**M**; Figure 5A), which expands to a more complex multiplet in the ^1H-coupled spectrum (Figure 5B). This resonance is phosphine concentration-dependent—adding more phosphine lessens the intensity relative to signal **K**. In addition, the **1** → **2** cyclization helps to clarify this assignment. After the **1** → **2** cyclization is complete, removal of all solvent and excess phosphine, followed by redissolution of the residue, affords a room-temperature spectrum with a similar chemical shift. Although no measurable coupling can be observed from the multiplet shown in Figure 5, the residue from the cyclization of **1** → **2** exhibits a triplet (J = 56 Hz) in the $^{31}P\{^1H\}$ NMR spectrum, and this resonance expands to a triplet of doublets (J_1 = 123 Hz, J_2 = 56 Hz) in the ^1H-coupled spectrum. This confirms the presence of two equivalent Y^{3+} centers and two phosphido ligands. We therefore assign this resonance to structure **M**. The crystal structure of the R = phenyl analogue is described in detail below.

M R = *n*-pentyl

A mixture of $(Cp'_2YH)_2$ and $PhPH_2$ was examined in the same manner and at −80 °C afforded spectra very similar to those shown in Figure 5. As the temperature is increased to room temperature, resonances analogous to **K**, **L**, and **M** decrease in intensity, and two new doublets grow in at δ −37.5 (dd, J_1 = 384 Hz, J_2 = 51 Hz) and δ −81.6 (dd, J_1 = 384 Hz, J_2 = 45 Hz), with the δ −37.5 ppm resonance exhibiting ^1H coupling in the ^1H-coupled spectra (J = 302 Hz), however, but no ^1H coupling is observed to the δ −81.6 resonance. The signals increase in intensity relative to the free phosphine signal as the temperature is raised further (up to 60 °C), and do not diminish in intensity upon cooling, indicating irreversible formation of a new species. A new doublet of doublets in the ^1H spectrum at δ 5.56 (J_1 = 302 Hz, J_2 = 11 Hz) is observed, and a singlet indicating formation of H_2 is also seen. A similar species is formed in the reaction of $(Cp'_2YH)_2$ and *n*-pentylphosphine, but is formed much more slowly at comparable temperatures. The very large coupling constant argues for a P−P bond,[56] and the

observation of two distinct phosphorus nuclei, one coupled to a proton, implies a structure such as **N**.[57]

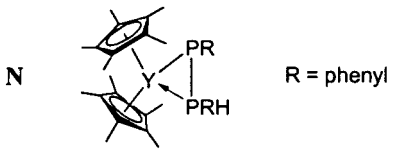

The low-temperature reaction of $(Cp'_2YH)_2$ + phosphinoalkene **1** presents a more complex picture, since two doublets with similar intensities are observed in the initial $^{31}P\{^1H\}$ NMR spectrum at −80 °C (δ −33.7, J = 110 Hz; δ −39.4, J = 68 Hz); both doublets also exhibit observable P−H couplings in the ^1H-coupled spectrum of J = 206 and 272 Hz, respectively. These resonances indicate likely coordination of a secondary phosphine (the side product phosphorinane) to the Y center at −80 °C. Although any phosphido resonance immediately analogous to **K** in Figure 5 is not detected, a phosphine−phosphido structure such as **O** seems most reasonable.[58]

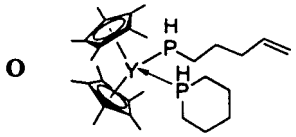

After allowing the cyclization of **1** → **2** to proceed to partial completion and then recooling the sample to −80 °C, two additional doublets (δ −20.3, J = 70 Hz; δ −24.1, J = 124 Hz) are observed; both doublets also exhibit P−H couplings in the ^1H-coupled spectrum, J = 267 and 205 Hz, respectively, and all four doublets have similar intensities. These new features indicate binding of the product phospholane to the catalyst as well. The large number of peaks indicates that several structures are present, including type **O** and also a structure such as **P**. As the temperature is raised, all of these resonances broaden and decrease in intensity, suggesting rapid interchange of free phosphine, free cyclized phosphorinane, and free cyclized phospholane in the resting state of the catalyst at temperatures above −20 °C.

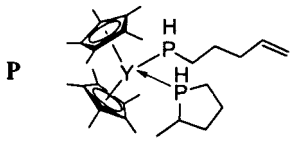

Molecular Structure of $[Cp'_2YP(H)Ph]_2$ (20). To understand more fully the various solution-phase species detected by ^1H and ^{31}P NMR, and to obtain further information on the catalyst resting state, attempts were made to crystallize a Ln−phosphido species. The molecular structure of the product of the reaction of $(Cp'_2YH)_2$ + $PhPH_2$ **20** (see Experimental Section for isolation and characterization procedures) was determined by low-temperature single-crystal X-ray techniques. The result is a high-symmetry dimer of the well-documented type $[Cp'_2Ln(\mu\text{-}X)]_2$, where in this case X = P(H)Ph (Figure 6; pertinent metrical parameters for the present structure are summarized in Table 6). This structure type has some precedent in Ln−N[59] and Ln−P[60] compounds, and examples of M_2P_2 dimers for Group 4 metals with primary and secondary phosphines are also known.[61] Because of the high symmetry of the structure, all Y−P distances are equal, 3.021(3) Å. This magnitude is, not unexpectedly, greater than typical two-center Y−P dative bonds (e.g., in **J**, Y−P1 = 3.005(3) Å, Y−P2 = 2.817(3) Å, Y−P3 = 2.896(3) Å, Y−P4 = 2.903(3) Å).[53a,62] In actuality, two of the four Y−P bonds in **20** must be formally dative, because the metal center is in the 3+ oxidation state. The ^1H NMR spectrum of **20** exhibits broad P−H signals at room temperature and above:[63] however, at −20 °C a doublet of doublets is

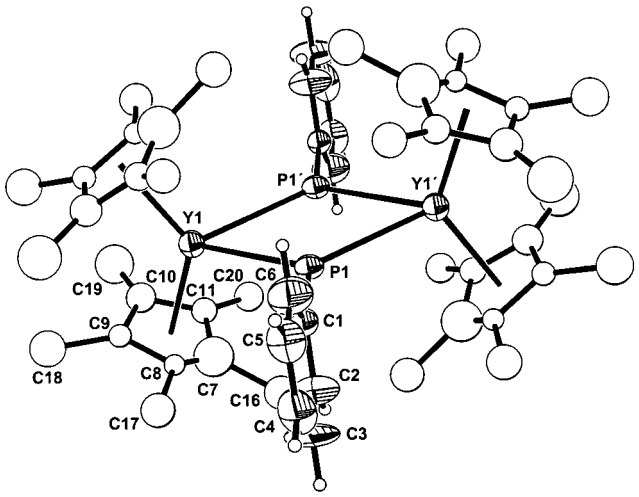

Figure 6. Molecular structure of $[Cp'_2YP(H)Ph]_2$ (**20**). Thermal ellipsoids are drawn at the 50% probability level. Carbon atoms on the Cp′ rings were refined isotropically.

Table 6. Selected Bond Distances (Å) and Angles (deg) for $[Cp'_2YP(H)Ph]_2$ (**20**)

Bond Distances					
Y1	P1	3.021(3)	P1	C1	1.86(2)
C1	C2	1.35(2)	C2	C3	1.37(3)
C3	C4	1.36(3)	C4	C5	1.31(3)
C5	C6	1.40(2)	C1	C6	1.40(2)
Y1	C7	2.68(2)	Y1	C8	2.63(2)
Y1	C9	2.66(3)	Y1	C10	2.64(3)
Y1	C11	2.66(3)	C7	C16	1.66(3)
C8	C17	1.56(4)	C9	C18	1.57(4)
C10	C19	1.58(4)	C11	C20	1.55(4)

Bond Angles			
P1−Y1−P1'	60.4(1)	Y1−P1−Y1'	119.6(1)
Y1−P1−C1	120.20(7)	C_g1^a−Y1−C_g2^a	130.6(7)

[a] C_g = ring centroid.

(56) In L_nMP_2 complexes, P−P coupling constants are typically greater than 300 Hz; for examples see: (a) Etkin, N.; Benson, M. T.; Courtenay, S.; McGlinchey, M. J.; Bain, A. D.; Stephan, D. W. *Organometallics* **1997**, *16*, 3504−3510. (b) Ho, J.; Breen, T. L.; Ozarowski, A.; Stephan, D. W. *Inorg. Chem.* **1994**, *33*, 865−870.

(57) This type of structure has some precedent in titanocene chemistry; see ref 61a.

(58) The difference in observed ^{31}P chemical shifts for the phosphido resonance of **O** vs that of **K** may reflect cyclic phosphine coordination to the metal in **O**. This could donate more electron density than a linear phosphine and therefore affect the resonance position of the linear phosphido ligand.

(59) (a) $[(MeC_5H_4)_2Yb(\mu\text{-}NH_2)]_2$: Hammel, A.; Weidlein, J. *J. Organomet. Chem.* **1990**, *388*, 75−87. (b)$\{(C_5H_5)_2Y[\mu\text{-}\eta^2\text{-}(HC{=}N^tBu)]\}_2$: Evans, W. J.; Meadows, J. H.; Hunter, W. E.; Atwood, J. L. *J. Am. Chem. Soc.* **1984**, *106*, 1291−1300.

(60) $(C_5H_5)_2Lu(\mu\text{-}PPh_2)_2Li(tmed)$: Schumann, H.; Palamidis, E.; Schmid, G.; Boese, R. *Angew. Chem., Int. Ed. Engl.* **1986**, *25*, 718−719.

(61) a) $[Cp_2Ti(\mu\text{-}P(H)Cy)]_2$: Xin, S.; Woo, H. G.; Harrod, J. F.; Samuel, E.; Lebuis, A.-M. *J. Am. Chem. Soc.* **1997**, *119*, 5307−5313. (b) Ho, J.; Drake, R. J.; Stephan, D. W. *Organometallics* **1993**, *12*, 3145−3157. (c) $[Cp_2Zr(\mu^2\text{-}PCyH)]_2$: Ho, J.; Stephan, D. W. *Organometallics* **1991**, *10*, 3001−3003.

(62) For other crystal structures containing Y−P bonds, see: (a) Karsch, H. H.; Graf, V.; Reisky, M.; Witt, E. *Eur. J. Inorg. Chem.* **1998**, 1403−1406. (b) Fryzuk, M. D.; Love, J. B.; Rettig, S. J. *J. Am. Chem. Soc.* **1997**, *119*, 9071−9072. (c) Fryzuk, M. D.; Love, J. B.; Rettig, S. J. *Organometallics* **1992**, *11*, 2967−2969.

resolved (δ 3.46, J_1 = 129 Hz; J_2 = 76 Hz), indicating both $^1J_{P-H}$ coupling and $^3J_{P-H}$ coupling.[64] Although the ^{31}P NMR resonance is too broad to resolve P−H coupling, the location at δ −107 agrees with the assigned dimeric structure type **M** (vide supra, R = phenyl).[65] The location of the H atoms in the structure is not clear, however since the two phenyl groups in the highly symmetric structure reside in only one plane, the two most likely positions are as drawn in **Q** and **R**.[66] This dimeric structure is somewhat different than the diffraction-characterized amine−amido complex, $Cp'_2La(NHCH_3)(NH_2CH_3)$ (**S**),[11a] which is related by Lewis base ring-opening of an analogous $[Cp'_2La(NHCH_3)]_2$ dimer. In the present case, the isolation of **20** apparently reflects, under the reaction conditions, greater stability and lower solubility of a dimer versus a phosphine−phosphido complex.

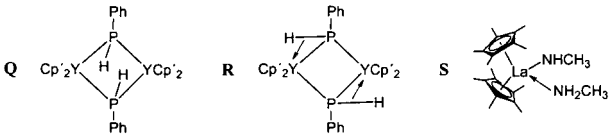

Discussion

Scope of Organolanthanide-Catalyzed Hydrophosphination/Cyclization. The goal of this research was to explore the viability and scope of organolanthanide-mediated intramolecular hydrophosphination/cyclization. The results in Table 2 indicate that $Cp'_2LnCH(TMS)_2$ complexes are effective precatalysts for the formation of five-membered (phospholane) and six-membered (phosphorinane) heterocycles with a variety of alkyl and aryl substituents. The reaction is efficient for both phosphinoalkenes and phosphinoalkynes, paralleling previous work for organolanthanide-catalyzed hydroamination of aminoalkenes[11] and aminoalkynes.[12] Although the cyclic products derived from phosphinoalkyne precursors undergo secondary reactions, products derived from phosphinoalkene cyclizations are stable and have potential uses as building blocks for known and new phosphine ligands.[18] The organolanthanide catalysts remain active, and turnover continues, as long as the reaction medium remains free of air and moisture. Further addition of substrate to a completed reaction mixture results in re-commencement of turnover and formation of additional cyclized product.

Both primary and secondary phosphines undergo cyclization; however, rates are modest for secondary phenylphosphines. Attempts to study cyclization selectivity with these more encumbered substrates (Table 2, entry 8) were thwarted by the low reaction rates, and furthermore, cyclization rates are surprisingly insensitive to geminal dimethyl substitution (the Thorpe−Ingold effect,[67] entry 9). However, the cyclizations of primary phosphinoalkenes are significantly more rapid and more informative. With regard to rates, the turnover frequency for the **3** → **4** transformation is significantly greater than that for **1** → **2** (Table 2) and indicates that in the proposed seven-membered pseudo-chair transition state (vide infra), the methyl substituent of **3** actually enhances the rate of cyclization. The greater **5** → **6** cyclization rate versus **1** → **2** is surprising, given that increased ring size normally correlates with depressed aminoalkene, aminoalkyne, and aminoallene hydroamination/cyclization rates[11−13] and also considering that process **7** → **8** is slower than **3** → **4**, and process **11** → **12** is slower than **9** → **10** (Table 2). The difference between ring-size effects for hydroamination and hydrophosphination must lie in the transition state and will be discussed in a following mechanistic section.

Metal and Ancillary Ligand Effects on Catalyst Activation and Activity. The ability to control the coordination sphere by varying metal ionic radius and ancillary ligation and consequently, ground-state and transition-state ligand−ligand and substrate−ligand nonbonded interactions, is one intriguing feature of homogeneous organolanthanide catalysis.[1] Accordingly, $Cp'_2LnCH(TMS)_2$ catalysts with the following six-coordinate ionic radii: Ln = La^{3+} (1.160 Å), Sm^{3+} (1.079 Å), Y^{3+} (1.019 Å), and Lu^{3+} (0.977 Å),[2] were examined in the present study. As the metal-ion size is decreased, the rate of protonolytic activation of the $Cp'_2LnCH(TMS)_2$ precatalyst (Scheme 2, step *i*) slows dramatically as judged by coordinated $-CH(TMS)_2$:dissociated $CH_2(TMS)_2$ ratios in the ^{1}H NMR. For example, a ∼30:1 ratio of **11**:$Cp'_2LaCH(TMS)_2$ at mM concentrations undergoes complete La−$CH(TMS)_2$ protonolysis in under 60 min at 25 °C. However, a 30:1 ratio of mM **19**:$Cp'_2YCH(TMS)_2$ does not undergo complete protonolysis even after 12 h at 25 °C. It is difficult to compare these results to the analogous precatalyst activation in hydroamination, because at −78 °C, protonolysis of the Ln−C bond is essentially instantaneous for solutions of comparable concentrations.[11] If Ln−C protonolysis of $Cp'_2YCH(TMS)_2$ with a primary amine is assumed to require ∼1 s, as compared to ∼12 h with the analogous phosphine substrate, then Ln−C cleavage is at least 5×10^4 times faster for amines than for phosphines. Because of this slow initiation step, most hydrophosphination reactions were carried out by first activating the catalyst with H_2 in situ[5a] and then adding the phosphine substrate to the resulting organolanthanide hydride.

The two different classes of phosphine substrates studied exhibit different reactivity trends with respect to variation of metal ionic radius and ancillary ligation and therefore will be discussed separately. For phosphinoalkynes, the hydrophosphination/cyclization reaction rate increases with increasing Ln^{3+} ionic radius, analogous to the trend observed for aminoalkenes[11] but opposite to that observed for aminoalkynes (Table 3).[12] For aminoalkynes, the very large exothermicity estimated for the insertion step (Scheme 1, step *ii*) was postulated to correlate with a more reactant-like transition state, and therefore less sensitivity to metal-ionic radius and structure of ancillary ligands.[12] For phosphinoalkynes, other factors are likely operative and are based on differences in the heteroatom, in that the softer and larger P forms significantly longer[68] and weaker[19]

(63) The broadening of the peaks suggests the dimer may be in equilibrium with a monomeric species at room temperature.

(64) The most likely cause of the second splitting observed in the ^{1}H NMR is $^3J_{P-H}$ or $^2J_{P-P}$ coupling, because Y−P−H couplings are expected to be very small (see ref 55). The observed coupling of 76 Hz is significantly greater than typical $^3J_{P-H}$ values. However, for coupling across a lanthanide metal center, two-bond P−Ln−P couplings are reported to be as large as 50-80 Hz (e.g., in structure **J**[a]), so that a large three-bond H−P−Y−P coupling constant is reasonable. For examples of $^3J_{P-H}$ couplings across a metal center, see: (a) Grobe, J.; Grosspietsch, T.; Le Van, D.; Krebs, B.; Läge, M. *Z. Naturforsch. B* **1993**, *48*, 1203−1211. (b) Fryzuk, M. D.; Joshi, K.; Chadha, R. K.; Rettig, S. J. *J. Am. Chem. Soc.* **1991**, *113*, 8724−8736. For examples of $^2J_{P-P}$ couplings across a metal center, see: (c) Bleeke, J. R.; Rohde, A. M.; Robinson, K. D. *Organometallics* **1995**, *14*, 1674−1680. (d) Bleeke, J. R.; Rohde, A. M.; Robinson, K. D. *Organometallics* **1994**, *13*, 401−403.

(65) In addition, the structure of **20** confirms the absence of a P−P bond, because the P−P distance in the crystal is 3.040(3) Å, whereas typical P−P bond distances are ∼2.2 Å. See Cowley, A. H. *Compounds Containing Phosphorus−Phosphorus Bonds*; Dowden, Hutchinson, and Ross, Inc.: Straudsburg, 1973; pp 1−9.

(66) A Pd−H−P interaction is suggested in the complex $[Pd_2(\mu\text{-}P^tBu_2)(\mu\text{-}PH^tBu_2)(PH^tBu_2)_2]^+$, see: Leoni, P.; Pasquali, M.; Sommovigo, M.; Laschi, F.; Zanello, P.; Albinati, A.; Lianza, F.; Pregosin, P. S.; Rüegger, H. *Organometallics* **1993**, *12*, 1702−1713.

(67) Kirby, A. J. *Adv. Phys. Org. Chem.* **1980**, *17*, 183−278.

Scheme 4. Possible Pathways for Insertion and Cyclization of Phosphinoalkenes

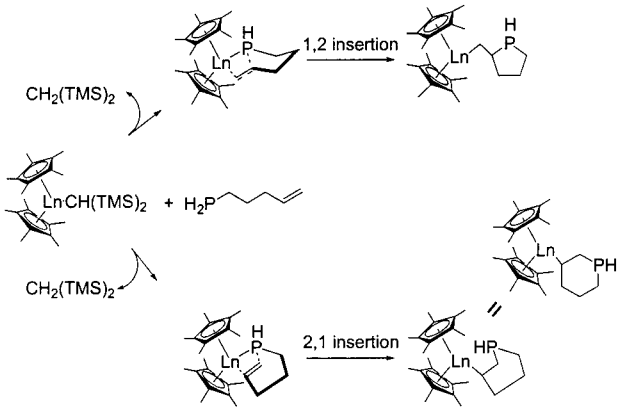

bonds to the metal center than N. That the rate of phosphinoalkyne cyclizations increases in the presence of more open supporting ligand systems (Table 2, entry 5, Cp'_2Sm-: N_t = 2.0 (40°) vs CGCSm−: N_t = 13.5 (22 °C)) is consistent with the aforementioned ionic radius effects and is again analogous to aminoalkenes.[3a] Similar metal-ionic radius and ancillary ligand effects are also qualitatively observed with other phosphinoalkynes, so that the effects observed are self-consistent within this class of substrates.

Phosphinoalkene cyclizations exhibit different reactivity trends with metal and ancillary ligands than do those of phosphinoalkynes. Variation of Ln^{3+} for Cp'_2Ln- catalysts reveals that the intermediate-sized Y^{3+} effects the highest turnover frequencies, with an overall progression $Y^{3+} > Lu^{3+} > Sm^{3+} > La^{3+}$ (Table 3). This appears to reflect an interplay of the weaker Ln−P bond vis-à-vis the Ln−N bond, and also the lower steric accessibility of the C═C bond versus the C≡C bond. It appears that turnover is most rapid when the "fit" between metal, substrate, and ligands is optimal. Very low rates for phosphinoalkene cyclization are also qualitatively observed with more open ligation, such as CGC ligands and chiral $Me_2Si(Cp'')(CpR^*)$ ligands. The lower rates with larger metal ions and more open coordination spheres may also be correlated with a larger number of coordinated phosphine substrate and product molecules in the catalyst coordination sphere (i.e., $Cp'_2Ln(PHR)(PH_2R)_n$, where $n > 1$) while for smaller ions, other phosphine ligands are less likely to access the catalyst and interfere with the cyclization. The Cp'_2Y- catalyst consistently exhibits the highest turnover frequencies for all phosphinoalkenes cyclized, so that once again catalyst effects are constant within a class of similar substrates.

Another unusual aspect of the **1** → **2** and **3** → **4** transformations is the occasional but in some cases substantial formation of an endocyclic six-membered ring (eq 1). This product becomes kinetically competitive when the substrate-catalyst "fit" is not optimal, such as for the large La^{3+} ion and the more open CGC ligand system, where the hydrophosphination/cyclization rate is slow. In these specific cases, the competing six-membered ring formation is significantly more rapid than if there were no catalyst present, suggesting that an alternate cyclization mechanism may be operative. Since all data indicate an irreversible insertion of the double bond, any reinsertion/skeletal isomerization pathway of **2** to a six-membered ring seems unlikely,

(68) In $Nd[N(TMS)_2]_3$, for example, the Nd−N bond length is 2.29(2) Å, see Andersen, R. A.; Templeton, D. H.; Zalkin, A. *Inorg. Chem.* **1978**, *17*, 2317−2319. In the similar compound $Nd[P(TMS)_2]_3(THF)_2$, the Nd−P bond length is 2.82(3) Å, see Rabe, G. W.; Ziller, J. W. *Inorg. Chem.* **1995**, *34*, 5378−5379.

Table 7. Activation Parameter Comparison for Hydrophosphination and Hydroamination

substrate	$\Delta H^{\ddagger}$, kcal/mol	$\Delta S^{\ddagger}$, eu
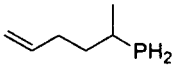	12.3 (1.6)	-25.9 (5)
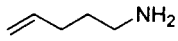	12.7 (1.4)	-27.0 (5)
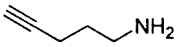	10.7 (8)	-27.4 (6)

an endocyclic insertive pathway such as that set forth in Scheme 4 cannot be rigorously ruled out. Although the proposed 2,1-insertion does not appear to be conformationally facile, it might be facilitated by the greater Ln−P and C−P bond lengths versus Ln−N and N−C bond lengths, as well as the more constricted C−P−C versus C−N−C bond angles.[69] Although 1,2-additions are observed in most lanthanide-mediated catalytic processes, there are examples in which competing 2,1-additions are also observed (e.g., eq 6).[7c] The present alternative insertion regiochemistry is only operative for substrates **1** and **3** and only in cases where the "fit" is not optimal[70] and is a plausible explanation for the observed formation of the endocyclic six-membered ring.

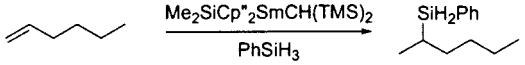

(6)

76% 2, 1 regioselectivity at 23° C

Kinetics and Mechanism of Hydrophosphination/Cyclization. The cyclizations reported here exhibit initial zero-order kinetics in substrate concentration (Figure 2) and first-order kinetics in catalyst concentration (Figure 3). These data imply that the same basic pathway is operative as was observed for catalytic hydroamination/cyclization,[11−13] with turnover-limiting insertion of the C−C unsaturation into the Ln−heteroatom bond, followed by rapid Ln−C protonolysis to afford the product heterocycle and regenerate the metal−heteroatom bond (Schemes 1, 2). Although, as noted above, the protonolysis of the initial precatalyst by phosphine substrates is substantially slower than that observed for amines (step *i*), this lower protonolytic reactivity does not affect the observed catalytic cycle and derived rate law in a major way. The protonolysis of the cyclized heterocycle Ln−C linkage by substrate (step *iii*) should be sterically more facile than initial $Ln-CH(TMS)_2$ protonolysis, and, judging from the findings for hydroamination, may well be intramolecular.[11a] Thus, the insertion of the carbon−carbon unsaturation into the metal−heteroatom bond (step *ii*) remains the turnover-limiting step in the catalytic cycle under typical reaction conditions.

For structurally similar substrates, the hydrophosphination/cyclization activation parameters are identical within experimental error to those for aminoalkene hydroamination (Table 7).[11a,12b] Considering the disparities in the energetics[19] of bonds being broken ($D(Sm-PR_2)$ = 36 kcal/mol vs $D(Sm-NR_2)$ = 52 kcal/mol; $D(R_2P-H)$ = 77 kcal/mol vs $D(R_2N-H)$ = 100

(69) sp^3-sp^3 C−N bonds average 1.47 Å, while P−C bonds average 1.84 Å; the C−P−C bond angles of PMe_3 are 98.3°, while the C−N−C bond angles in NMe_3 are 106°; see Gilheany, D. G. *The Chemistry of Organophosphorus Compounds*; Hartley, F. R., Ed.; Wiley: Chichester, 1990; Vol. 1, pp 9−49.

(70) It is interesting that this side reaction is not observed for hexenyl substrates **5** and **7**, but not completely surprising since they would form less kinetically favored seven-membered rings.

kcal/mol) and formed ($D(R_2P-CH_3 = 63$ kcal/mol vs $D(R_2N-CH_3 = 80$ kcal/mol) as the respective hydroamination and hydrophosphination reaction coordinates are traversed, there are remarkable overall energetic similarities for the two processes. For both processes, there is a relatively modest enthalpic barrier, suggesting a concerted transition state with significant bond formation compensating for bond-breaking. The large negative hydrophosphination entropy of activation indicates a highly ordered transition state, similar to that postulated for hydroamination (**T**, X = N), for example, a seven-membered chairlike conformation in the case of pentenyl phosphines (**T**, X = P).

T

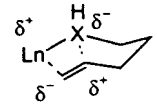

In the present study, cyclization rates for closure of five- and six-membered phosphorus-containing rings are found to be similar, instead of observing a clear 5 > 6 trend as in the case of amines (eqs 7, 8).[11,12] Ring-strain differences for five- and six-membered rings are expected to be small,[71] and low-level AM1 and PM3 calculations show that ΔH_f for homologous phosphorus- and nitrogen-containing heterocycles are approximately equal. Therefore, complex and subtle factors in the transition state for hydrophosphination must play a role in determining the rates of ring closure versus the size of the ring. Factors causing the deviation from hydroamination trends are likely to include differences in N versus P hardness and softness,[42] differences in Ln−N, N−C versus Ln−P, P−C ground-state bond lengths and angles,[69] and differences in conformational mobility of N versus P heterocycles (phosphorus-containing heterocycles are generally less mobile).[72]

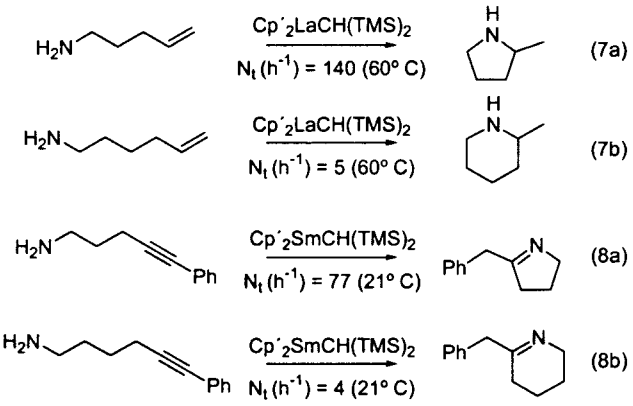

Diastereoselectivity of Hydrophosphination/Cyclization. As noted above, the cyclization **3** → **4** exhibits increasing product *trans*-diastereomer selection with increasing Ln^{3+} ionic radius (Table 4, entry 2, excluding Cp'_2La-mediated reactions which proceed principally via the Scheme 4 endocyclic pathway). The increase in the *trans* ring closure selectivity can be explained using the same argument used to explain *trans*:*cis* selection processes in formation of *trans*-rich 2,5-dimethylpyrollidine from 1-methyl-pent-4-enylamine (analogous to the present **3** → **4** cyclization).[10a] With the (comparatively) larger Cp'_2Sm- catalyst center, the coordination of other phosphine bases is likely more probable, leading to a more crowded transition state and forcing the proximate methyl substituent into an equatorial disposition, thus leading to a *trans*-rich product (Scheme 5). The more congested Cp'_2Y- and Cp'_2Lu- catalysts centers would discourage participation by other bases, leading to a less congested transition state, which allows the more sterically demanding axial orientation of the methyl group and favors formation of the *cis*-rich product. A similar steric/stereochemical effect was also observed in aminoalkene cyclizations, and in these studies, increased congestion caused by addition of other bases (e.g., *n*-propylamine) led to an increased *trans*:*cis* product ratio.[11a] Adding *n*-propylamine to the present phosphine cyclizations is found to alter the catalyst/substrate interplay, in that large Ln^{3+} ions now exhibit *less* selectivity, while smaller Ln^{3+} ions afford *increased trans*:*cis* ratios (Table 4). In these cases, added amine likely binds more strongly to the metal center than the phosphine, perhaps biasing the cyclizing substrate toward the more favorable equatorial methyl group orientation. This *trans* selectivity effect increases as the metal ionic radius decreases, again indicating the high sensitivity of the phospholane ring closure stereochemistry to the surrounding steric environment.

Diastereoselectivity in the cyclization of other phosphine substrates is much less sensitive to the nature of the organolanthanide catalyst. Selectivity in the **1** → **2** cyclization is virtually catalyst-independent, indicating (as proposed above) that the additional methyl group of **3** must exert considerable influence on stereoselection in the transition state. Closure of larger rings (**5** → **6** and **7** → **8**) is also relatively insensitive to catalyst identity (Table 4), and the same is true for formation

Scheme 5. Effect of Metal Ionic Radius on Phospholane Ring-Closure Diastereoselectivity

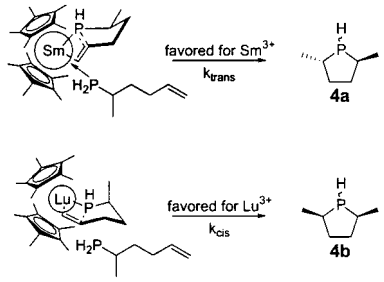

Table 8. Comparison of Organolanthanide-Mediated Hydroamination and Hydrophosphination

	Hydroamination	Hydrophosphination
Initial Lanthanide-Carbon Bond Protonolysis	immediate	slow; more effective to use $(Cp'_2LnH)_2$ precatalyst
Max. Turnover Frequency (h^{-1})		
H_2X	95 (Cp'_2La, 25° C)	50 (Cp'_2Y, 25° C)
H_2X, Ph	77 (Cp'_2Sm, 21° C)	13 (Cp'_2La, 22° C)
N_t as a function of Ln^{3+} radius		
alkenes	La > Sm > Y > Lu	Y > Sm > Lu > La
alkynes	Lu > Y > Sm > La	La > Sm > Y > Lu
Empirical Rate Law	$v = k[substrate]^0[catalyst]^1$ little/no inhibition by product seen	$v = k[substrate]^0[catalyst]^1$ inhibition by product seen after ~1 half-life
Isolable Catalyst Resting State	$Cp'_2Ln(NHR)(NH_2R)$	$[Cp'_2YP(H)Ph]_2$

(71) The difference in ring strain between five- and six-membered saturated hydrocarbon rings is ~6 kcal/mol, see: (a) Dudev, T.; Lim, C. *J. Am. Chem. Soc.* **1998**, *120*, 4450−4458. (b) Isaacs, N. S. *Physical Organic Chemistry*; John Wiley & Sons: New York, 1987, Chapter 8.

(72) For conformational mobilities of heterocyclic rings, see: (a) Gupta, R. R.; Kumar, M.; Gupta, V. *Heterocyclic Chemistry*; Springer: Berlin, 1998; Vol. 1, pp 129−146. (b) Lambert, J. B. *Top. Stereochem.* **1971**, *6*, 19−105.

of rings that are sterically more encumbered (**13** → **14**, **15** → **16**, and **17** → **18**).

Catalyst Resting State. The catalyst resting state, as surveyed using paramagnetic catalysts and variable temperature NMR spectroscopy, is rather complex. The labile Ln−P bonding affords more rapid exchange of free and bound substrate than was observed with amines, and this interchange is rapid on the NMR time scale down to −80 °C. With noncyclizable phosphines such as *n*-pentyl phosphine (**19**) or phenylphosphine, a Y−PHR phosphido bond is detectable; however, exchange of free and bound phosphines remains rapid on the NMR time scale. In addition, there is significant coordination of the product heterocycles to the metal center. This coordination is qualitatively assessed through broadening of the product P−H resonances in the presence of paramagnetic catalysts, and complexation is directly observed at low temperature during the Cp'_2Y-mediated cyclization of **1** → **2**. It is therefore clear that the cyclized phosphines participate in the catalyst resting state and perhaps are bound more strongly to the catalyst than linear substrate at low temperature. At room temperature, free linear phosphine, bound linear phosphine, and cyclized phosphine all interchange at rates far in excess of the catalytic turnover frequencies.

On the basis of the ^{31}P NMR data and the crystal structure of a species isolated from solution, a μ-PHR dimer (**M**; Figure 6) can be formed but is only present in significant concentrations at very low substrate:catalyst ratios, and at most catalytic concentrations does not make a significant contribution to the catalyst resting state. As the concentration of phosphine is increased, phosphine−phosphido complexes predominate, and the dimer is not present in significant concentrations. From the present results and those for the analogous organolanthanide−amine chemistry, the probable resting state of the catalyst under true catalytic conditions is a mixture of species such as **U** and **U'**.

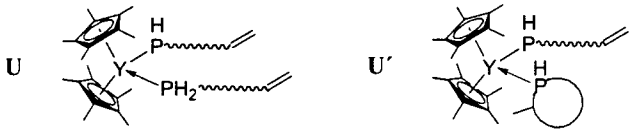

Hydroamination versus Hydrophosphination. Table 8 presents a comparison of organolanthanide-mediated hydroamination[11,12] and hydrophosphination processes. Slow generation of the active catalyst for phosphines versus amines represents a substantial difference between the two processes and is surprising when considering that this protonolytic reactions is more exothermic for phosphines than for amines (eqs 9a, 9b).[19]

$$Ln\text{-}CHTMS_2 + H\text{-}NR_2 \longrightarrow H\text{-}CH(TMS)_2 + Ln\text{-}NR_2 \quad \Delta H \sim -15\ kcal/mol \qquad (9a)$$

$$Ln\text{-}CHTMS_2 + H\text{-}PR_2 \longrightarrow H\text{-}CH(TMS)_2 + Ln\text{-}PR_2 \quad \Delta H \sim -22\ kcal/mol \qquad (9b)$$

These differences appear to reside in interplay of Lewis (initial binding to the Ln^{3+} center) and Brønsted (R_2PH species are more acidic than R_2NH)[43] acid−base interactions. Both alkenyl and alkynyl phosphines undergo cyclization, and the mechanism of the transformations is broadly similar to that of the analogous hydroaminations. Another similarity is in the maximum turnover frequencies of the cyclizations, with the rates of phosphine cyclizations generally of the same order of magnitude as the analogous hydroamination/cyclizations. Interestingly, phosphinoalkene maximum rates are greater than phosphinoalkyne maximum rates—the opposite of what is observed for hydroamination.[11,12] Thus, the heteroatom identity has a greater overall effect on the rates of the cyclization process than does the steric accessibility of the unsaturation. Turnover frequencies vary with metal-ionic radius and ancillary ligation in understandable ways for both hydroamination and hydrophosphination. Although competitive inhibition by cyclized product is more evident for phosphines than for amines, the experimental rate laws for the two processes are the same. Despite all of these differences between phosphorus and nitrogen, the cyclization activation parameters are surprisingly similar (Table 7). The resting state of the hydrophosphination catalyst is complicated, and at low ratios of substrate:catalyst a Ln_2P_2 dimer is evident, but at typical catalytic concentrations, the resting state appears to be similar to that postulated for hydroamination. Desirable *trans*-selectivity is at present not as high for the 2,5-dimethyl phospholane (**4a**) as for the analogous pyrollidine;[11] however, cyclizations with promising chiral organolanthanide catalysts are far more selective and will be reported elsewhere.[4c]

Conclusions

The present results show that intramolecular hydrophosphination/cyclization catalyzed by organolanthanides is a general reaction that can be used to construct a variety of phosphorus-containing heterocycles. The turnover frequencies and selectivities are highly dependent on lanthanide ion, ancillary ligands, and substrate, and trends are in some cases similar to, and in some cases very different from, those observed for analogous hydroamination/cyclization processes. A mechanism qualitatively similar to that previously defined for amine hydroamination/cyclization appears operative in the present catalytic systems.

Acknowledgment. Financial support by the NSF (CHE-0078998) is gratefully acknowledged. M.R.D. thanks Dr. Y. Wu for assistance with 2D and low temperature NMR experiments.

Supporting Information Available: An X-ray crystallographic file in CIF format for **20**. This material is available free of charge via the Internet at http://pubs.acs.org.

JA010811I